

**A FRAMEWORK FOR OPTIMAL DECISION MAKING OF A
PHOTOVOLTAIC RECYCLING INFRASTRUCTURE PLANNING**

Dissertation

Submitted to

The School of Engineering of the

UNIVERSITY OF DAYTON

In Partial Fulfillment of the Requirements for

The Degree of

Doctor of Philosophy in Engineering

By

Qi Guo

UNIVERSITY OF DAYTON

Dayton, Ohio

August, 2017

A FRAMEWORK FOR OPTIMAL DECISION MAKING OF A PHOTOVOLTAIC RECYCLING INFRASTRUCTURE PLANNING

Name: Guo, Qi

APPROVED BY:

Jun-Ki Choi, Ph.D.
Advisory Committee Chairman
Assistant Professor
Department of Mechanical and
Aerospace Engineering

Chuck Ebeling, Ph.D.
Committee Member
Professor Emeritus
Department of Engineering
Management, Systems, and
Technology

Ronald Deep, Ph.D.
Committee Member
Professor Emeritus
Department of Engineering
Management, Systems, and

Shuang-ye Wu, Ph.D.
Committee Member
Associate Professor
Department of Geology

Robert J. Wilkens, Ph.D., P.E.
Associate Dean for Research and Innovation
Professor
School of Engineering

Eddy M. Rojas, Ph.D., M.A., P.E.
Dean. School of Engineering

© Copyright by
Qi Guo
All rights reserved
2017

ABSTRACT

A FRAMEWORK FOR OPTIMAL DECISION MAKING OF A PHOTOVOLTAIC RECYCLING INFRASTRUCTURE PLANNING

Name: Qi Guo
University of Dayton

Advisor: Dr. Jun-Ki Choi

Solar energy, as an emerging renewable clean energy, has been rapidly growing for 15 years all over the world and is expected to grow 15% annually until 2020. In 2015, at least 40 GW of Photovoltaic (PV) systems were installed, achieving 178GW current solar power installation worldwide. In the next five years, 540 GW cumulative capacities are expected to be installed worldwide and US contributed 6.5 GW PV installations in 2015. US electricity demand is expected to be dominated by solar power by 2050 or even earlier. The widespread deployment of PV will not only contribute to a reduction in greenhouse gas emission, but can also mitigate the worldwide fossil fuel depletion.

As the number of PV systems increases, the mass of PV waste will increase as well, adding a new source to the existing waste stream. The amount of End-of-Life (EoL) PV will approach 13.4 million ton worldwide, including approximately 5.5 million ton located

in the US by 2025. PV contains high value, toxic, and energy-intensive materials. In addition, the market price of some materials utilized in the thin-film and crystalline PV technologies has drastically increased in the recent years.

There is a strong need of coordinating the information to optimize the reverse logistics planning in a photovoltaic (PV) recycling network in the U.S. Two major tasks are included: 1) locating PV Recycling Centers (PVRC); 2) allocating Transportation Companies (TC) shipping PV installation sites (PVIS) to PVRC. One contribution of this dissertation is to decide the optimal number, as well as the location of PVRC by minimizing the overall cost. Another contribution is to determine the optimal distribution scheme to minimize the transportation cost among TC, PVIS, and PVRC.

In order to accomplish the two tasks, a mathematical modeling framework was developed to facilitate PV recycling in an economically and environmentally feasible manner. The framework included two mathematical models: 1) Multi-Facility Optimization Model; 2) Optimal Distribution Model. The multi-facility optimization model included the transportation module, the economic module, and the environmental module. The model identifies the geographical location of the prospective PVRCs by minimizing the total costs in different scenarios. While in the Optimal Distribution Model, a static and a dynamic optimization algorithm was applied for conducting the optimal solution accurately and efficiently.

To show the efficacy of the proposed framework, case studies for recycling EoL PV in California were performed. Historical PV installation data in the region was utilized to gather information about the amount of the prospective end-of-life (EoL) PV waste generation in CA. In order to integrate the temporal and the spatial dispersion of PVISs in

CA, a three-phase recycling plan was proposed. For well displaying the geographical results, Geographic Information System (GIS) was utilized to visualize the installation data, optimized location of the PVRCs, and the optimal distribution scheme. The proposed generic framework provided a great insight for decision makers about the trade-offs among various scenarios by considering cost, environmental impact, and investment risk on PV recycling planning.

To my Dad and Mom,
I will not be able to have the educational opportunity
without all your support.

ACKNOWLEDGMENTS

First, I would like to express my sincerest appreciation to my PhD advisor Dr. Jun-Ki Choi. Thank you for giving me the opportunity to be a PhD your student. Thank you so much for all effort he you put towards my PhD study.

I also want to thank all my PhD committee members: Dr. Chuck Ebeling, Dr. Ronald Deep, and Dr. Shuang-ye Wu. Thank you so much for all the time and advise you provided towards my study.

My thanks also go out to all faculty and staff in the University of Dayton who helped me on my study.

TABLE OF CONTENTS

ABSTRACT.....	iv
ACKNOWLEDGMENTS	viii
LIST OF FIGURES	xii
LIST OF TABLES.....	xiii
LIST OF SYMBOLS	xiv
CHAPTER I. INTRODUCTION.....	1
1.1 The Global PV Market.....	1
1.2 Rationale for PV Recycling	2
1.3 Current Status of PV Recycling.....	3
1.4 Studies for Setting PV Recycling Infrastructure.....	5
1.5 Studies for Optimizing the Location of PVRC	6
1.6 Reducing Transportation Cost on PV Recycling.....	7
1.7 Optimization Algorithm: MILP, GA	9
1.8 Aim and Contribution	10
CHAPTER II. METROLOGY.....	11
2.1 PV Recycling Framework Overview	11

2.1.1 Creating Database for Input	13
2.1.2 Locating PVRC	13
2.1.3 Generating Distribution Scheme.....	13
2.1.4 Performing Trade-off Analyses	14
2.2 Uniqueness.....	15
2.2.1 Integrated Temporal and Spatial Dispersion of PVIS.....	15
2.2.2 Developed Multi-Facility Optimization Model	15
2.2.3 Developed Optimal Distribution Model	15
2.2.4 Employed GIS for PV Recycling Optimization.....	16
CHAPTER III. MULTI-FACILITY OPTIMIZATION MODEL	17
3.1 Transportation Module.....	17
3.1.1 Distance Definition	18
3.1.2 Distance in PV Recycling	19
3.1.3 Optimization Tool.....	22
3.1.4 Mathematical Model	24
3.1.5 Local and Global Minimum.....	25
3.1.6 Alternate Optimization Tool: GIS	28
3.2 Economic Module	29
3.3 Environmental Module	30
CHAPTER IV. CASE STUDY OF MULTI-FACILITY OPTIMIZATION MODEL	31

4.1 PV Installation Size, Type, and Location	31
4.2 Phase I: Short-term Planning	37
4.3 Phase II: Mid-term Planning.....	39
4.4 Phase III: Long-term Planning.....	42
4.5 GIS Optimization	45
CHAPTER V. OPTIMAL DISTRIBUTION MODEL	47
5.1 Model Description	47
5.2 Static Optimization Algorithm.....	49
5.3 Dynamic Optimization Algorithm	50
CHAPTER VI. CASE STUDY OF OPTIMAL DISTRIBUTION MODEL	52
6.1 Data Description	52
6.2 Optimization Algorithm Application.....	56
6.3 Results.....	58
CHAPTER VII. CONCLUSION AND FUTURE WORK.....	65
BIBLIOGRAPHY	68
APPENDIX A-1: Location of PVRC in Phase I.....	74
APPENDIX A-2: Location of PVRC in Phase II	75
APPENDIX A-3: Location of PVRC in Phase III	76
APPENDIX B: Large PVIS	77

LIST OF FIGURES

Figure 1.2: PV waste projection in the U.S.	2
Figure 2.1: Structure of the PV recycling framework.....	12
Figure 3.1: Demonstration of local minimum and global minimum.	26
Figure 4.1: Annual PV installations in California (1984 – 2016).....	32
Figure 4.2: Size of the installed PV during 1984 - 2015 in CA.....	36
Figure 4.3: Total system cost vs. number of PVRC in Phase I.....	38
Figure 4.4: Two PVRCs selected for Phase I (2021 - 2025).	39
Figure 4.5: Total system cost vs. number of additional PVRCs in Phase II.....	41
Figure 4.6: Six PVRC selected for Phase II (2026 - 2030).....	42
Figure 4.7: Total system cost vs. number of additional PVRCs in Phase III.	44
Figure 4.8: Six PVRCs selected for Phase III (2031 - 2035).....	45
Figure 5.1: Mechanism of recycling network	48
Figure 5.2: Mechanism of GA	50
Figure 6.1: Locations of PVIS and PVRC in each recycling period	53
Figure 6.2: Annual PV installations in California (1984 – 2015).....	55
Figure 6.3: Transportation cost and saving by each method and year.....	58
Figure 6.4: Distribution decision of year 2003, 2008, and 2013	63

LIST OF TABLES

Table 4.1: Number of sites and size of PVIS.....	34
Table 4.2: Total costs and emission generated from the Phase I planning.	37
Table 4.3: Total costs and emission generated from the Phase II planning.....	40
Table 4.4: Total costs and emission generated from the Phase III planning.	43
Table 4.5: Transportation distance by Matlab and GIS	46
Table 6.1: Total cost and multiple PVIS Size and quantity combination.....	60
Table 6.2: Saving of GA' and LP of each year.....	61
Table 6.3: Percentage saving of in each cost structure of each year.....	62
Table 6.4: Amount of EoL PV each PVRC receives each year.....	64

LIST OF SYMBOLS

Indices:

I	Set of all existing PVIS, $i \in I$
J	Set of PVRC, $j \in J$
K	Set of TC, $k \in K$
Φ	Latitude set of all PVRCs' latitude, $\phi \in \Phi$
Λ	Longitude set of all PVRCs' longitude, $\lambda \in \Lambda$

Parameters:

W_i	Weight of material of PVIS i
ϕ_j	Latitude of the PVRC j
λ_j	Longitude of the PVRC j
C_j	Max annual recycling capacity of PVRC j
C_k	Max annual transportation capacity of TC k
l	Max load of the transporting truck

n_i	The number of trips required to recycle the PVIS
D_{ij}	Distance between PVIS i and PVRC j
D_{ki}	Distance between TC k and PVIS i
D_{jk}	Distance between PVRC j and TC k
f_k	Fixed cost charged by TC k
m_k	Unit mileage cost charged by TC k
w_k	Unit weight cost charged by TC k

Decision variables:

X_{ij} PVIS i is shipped to PVRC j , where,

$$X_{ij} = \begin{cases} 1 & \text{if shipped} \\ 0 & \text{otherwise} \end{cases}$$

Y_{ijk} PVIS i is shipped to PVRC j by TC k , where,

$$Y_{ijk} = \begin{cases} 1 & \text{if shipped} \\ 0 & \text{otherwise} \end{cases}$$

CHAPTER I

INTRODUCTION

1.1 The Global PV Market

The market for photovoltaics (PV) has been growing world-wide during the last 15 years and is expected to continue growing at least by 15% annually until 2020 [1, 2]. In 2015, 50.6 GW new solar photovoltaics (PV) was installed worldwide. A 613 GW grid-connected solar power was forecasted by the end of 2019 all over the world. [3] In the United States, alone, a record 14.8 GW of PV capacity was added in 2016 bringing the total installed PV capacity to 78 GW and the industry is poised to increase to 100 GW over next five years. With the 39% renewable electric occupancy, Solar energy has become the No. 1 renewable electric energy in the United States in 2016. As the largest installer, in 2016, PV installation in California accounted for 35% amount of the United States. The cumulative PV installation in CA has researched 17 GW. [4] The widespread deployment of PV will not only contribute to a reduction in greenhouse gas emission, but can also mitigate the worldwide fossil fuel depletion [5, 6]. As the number of PV systems increases, the mass of PV waste will increase as well, adding a new source to the existing waste stream. The amount of End-of-Life (EoL) PV will approach 13.4 million ton worldwide, including approximately 1.8 million ton located in the US by 2025. Figure 1.1 illustrates a

preliminary PV waste prognosis based on the historical data of PV installation in the U.S [7]

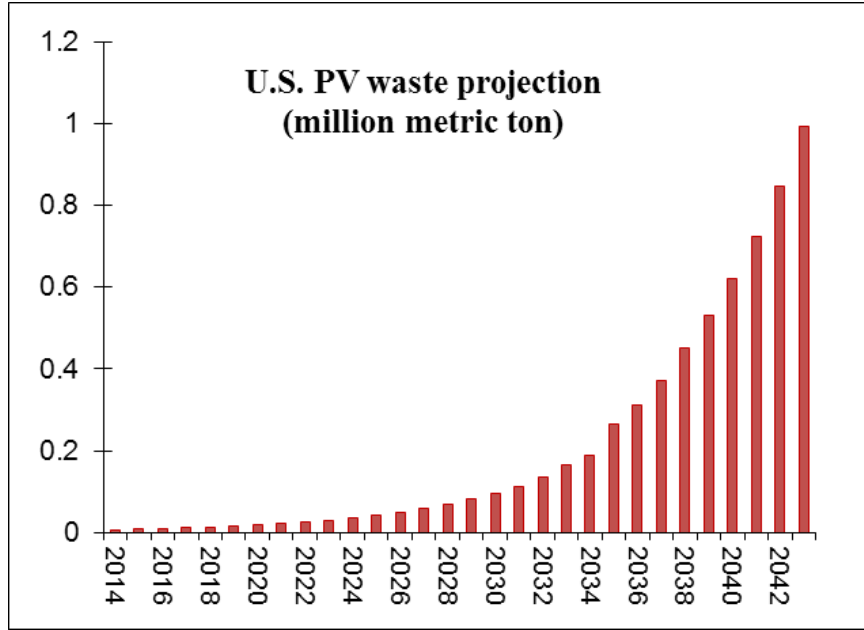


Figure 0.1: PV waste projection in the U.S.

1.2 Rationale for PV Recycling

PV contains valuable, hazardous, and energy-intensive materials. First, several high demand elements such as Se, Zn, Fe, and Ag are contained in PV. Those elements are the pillar of national industry [8]. Appropriately recycling those elements can eliminate the resource scarcity and material supply threat [9, 10], subsequently, stabilizing the security of the national economy. On the other hand, recycling the existing EoL PV can also partially evade the risk of material shortage or oversupply in PV manufacturing, smoothing the price fluctuation of the PV industry [11]. In addition, the market price of some materials utilized in the thin-film and crystalline PV technologies has drastically increased in the recent years [12, 13]. High profit is even expected to be achieved by recycling elements In

and Ga in CIGS PV, a type of thin-film panel [14, 15]. Second, PV contains tons of toxic elements such as As, Cd, and Se. As and Cd even have a 6 and 4 tenfold toxicity index over common elements such as Cu [16]. Those hazardous materials need to be reclaimed thoroughly to ensure the health of both the environment and human beings. Third, energy intensive components such as silicon wafers can be recovered during the pyrolysis by recycling the mono- and poly- crystalline PV [17]. In industry, producing 0.256 gram silicon wafers consumes 1,600 g secondary fossil fuel and 32,000 g water [18]. By implementing the recycling process, energy intensive materials, such as semiconductor elements, aluminum, and glass, can be retrieved effectively for remanufacturing of the CdTe and c-Si PV [11]. The technical and economic feasibility of the retrieving process has been verified by a previous researcher [19].

1.3 Current Status of PV Recycling

Although PV recycling technologies are available for both silicon and thin-film based modules [20, 21], the recycling process has not been deployed in most of countries due to the shortage of effective collection infrastructure and incentive policies. Cost effectiveness has been emphasized as the greatest challenge in employing and recycling of the PV system [22, 23]. Considering the potential trade-off among the cost factors is crucial for ensuring the sustainability of PV recycling. Previous studies showed that transporting reclaimed materials among stakeholders has enormous economic and environmental impacts on recycling planning [24, 25]. Choi and Fthenakis showed that the size of PVRCs should be optimized so that the annual incoming PV waste are processed economically[26]. However, our previous study did not include long-term end-of-life planning as it was intended to guide decisions for recycling of PV waste generated from current

manufacturing scraps. The economic feasibility of end-of-life recycling is debated and Cucciola et al. [10] reported that the annual capacity of a PV recycling plant should reach certain capacity in order to provide sufficient economic incentives in the recent PV installation rates in Italy. Goe et al. also concluded that the material recovery cost is more expensive than directly disposing based on the current technology and policies in the state of New York [27]. It is obvious that recycling is the most environmentally friendly approach to treat the retiring PV[28]. However, the economic feasibility of the recycling process is still under exploration. Confronting the rapid commercialization of the PV industry, the adoption of constructive policies such as imposing higher fee and taxes are vital to the retiring PV recycling process. There is also a need to appeal to stakeholders to get involved as much as possible [2, 27].

In Europe, recycling of EoL electronic goods is regulated by the Waste Electrical and Electronic Equipment (WEEE) Directive. The directive included PV and required all PV module manufacturers who sell in EU countries to have recycling programs in place [29, 30]. The industry had initiated the voluntary program with PVCYCLE in 2010, which now oversees compliance with the WEEE [31]. In the U.S., there are no policies yet directly related to the development of PV recycling and with no legal obligations to process waste, cost optimization of recycling is imperative for the industry to voluntarily undertake such initiative. Because reverse logistics networks are complex, a systematic approach is needed to capture the dynamic interactions among stakeholders that would minimize the cost to the industry and ideally make end-of-life PV recycling a profitable operation. This entails with data analysis to identify the optimal locations for Photovoltaic Recycling Centers

(PVRs) so that the sum of the costs associated with the reverse logistics the capital cost of collection and recycling facilities are minimized.

1.4 Studies for Setting PV Recycling Infrastructure

Some EoL PV recycling infrastructure have been proposed by previous researchers. Fthenakis devised a recycling infrastructure to demonstrate the feasibility of thin-film solar cells recycling. In that infrastructure, both the centralized and decentralized scenarios were discussed with the quantitative parameters included [17]. Considering the complexity of the recycling process in collection and transportation aspects, a mathematical framework is recommended to resolve the PV recycling problem [32]. In that paper, they took the thin-film PV as an example, demonstrating an operational recycling framework to take back the EoL PV that manufactured by the company of First Solar. The same author also published their mathematical model regarding the economic feasibility to recycle the EoL crystalline silicon PV in both macro and micro perspective in Germany [2, 26]. Cucchiella, etc, provided a financial analysis of recycling the EoL PV modules in Italy by considering the factors of technology, environment, and economy, as well as a sensitivity analysis between these factors [10]. Goe etc. performed a tradeoff analysis between multi-criteria by using both mathematical method and Geographical Information System (GIS) selection tools to research the optimal location to site the PV recycling centers in the state of New York [27].

There is also literature available regarding the characteristic and construction of reverse logistics networks based on recovering other products [33-36]. Most studies are limited to investigating solutions for economic feasibility on the EoL management of the electronic appliances and information technology (IT) products such as computer, monitor, laptop, and cellphone. The fast turnover of consumer electronics creates a large waste stream of

obsolete electronic waste, providing opportunities to establish a relatively stable and economically viable recycling infrastructure.

Unlike electronic products, it takes time for PVs to accumulate sufficient waste modules because of the decades-long intervals between installing and discarding them. The PV market has increased exponentially, therefore, the capacity of PVRCs needs to be strategically planned to process the exponential growing numbers of end-of-life (EoL) PV modules considering spatial and temporal factors. Sizing the initial capacity of the expected PVRCs in an economic manner is crucial in short-term period planning. In the mid- and long-terms, existing PVRCs could expand the processing capacity or new PVRCs should be added to the new geographical location in the region to be able to process growing amount of EoL PV modules. Therefore, in order to make the PV recycling economical, the quantity, the annual capacity, as well as the locations of PVRC needs to be determined for each recycling term. In addition, the distribution scheme needs to be optimized to while transporting PVIS to PVRC.

1.5 Studies for Optimizing the Location of PVRC

There are several proposed models on facility location optimization [33-37]. A Lagrangian experimental model was employed for optimizing a facility location problem with large geographical scale variables and capacity constraints [38]. Other studies have solved location optimization problems by decomposing the problem into multiple single facility problems [39-43]. These quantitative modeling schemes suggested efficient levels of the reverse logistics and supply chain management. Effendigil et al. [44] proposed a framework which employs artificial neural networks and fuzzy analytical hierarchy process in order to assure the maximum profitability of reverse logistics planning.

Approaches to location allocation problems have been studied, specifically for the PV recycling case. Choi, etc. performed a location optimization for the PV recycling facilities among a finite set of locations with a short-time of 5 years based on the current PV installation situation in Germany. Minimizing the total travel distance is the objective of that optimization. Capacity limitation of each recycling center and other realistic restrictions were considered as constraints in that model. CPLEX was employed as the optimization solver to generate solutions [26]. These authors reiterated the supremacy of appropriately allocating the PV recycling facility while recommending the recycling scheme for the First Solar Company: the most favorable scenario was expected to save \$107,000 per month, while a \$151,000 loss was anticipated every month in the least profitable scenario [32]. There were also location allocation models performing the recycling process for other products. Louwers developed a location allocation framework to collect, preprocess, and redistribute carpet waste with complete flexibility on location selection. Their networks were employed both in Europe based on the supply-driven reuse and in the United States based on the demand-driven reuse [39].

1.6 Reducing Transportation Cost on PV Recycling

Reducing the transportation cost is another operative aspect to reduce the PV recycling expense. In order to make the recycling affordable and profitable, the recycling process and the system cost throughout the entire collection, distribution, and transportation need to be optimized and minimized, respectively [45]. The PV reverse logistics cost, a cost for collecting and transporting the EoL PV modules, can be minimized by appropriately selecting the optimal location of PV recycling centers [2]. In that research, the author concluded that the reverse logistics cost is the leading cost among the entire PV recycling

process. When Goe etc. conducted the retiring PV recovery in the state of New York, they considered the transportation cost as an indispensable parameter in their material recovery framework as well [27]. The predominance of the reverse logistics cost was also emphasized while performing a financial analysis to the EoL PV modules in other literature [10].

Implementing mathematical optimization is an effective way to reduce the transportation cost. Classical mathematical optimization models of the vehicle routing for the facility location decision has been summarized [46]. A waste collection optimization was performed by minimizing the route distance. A modified Backtracking Search Algorithm was applied in the capacitated vehicle routing problem models. By optimizing, the average waste collection efficiency was improved by 37%, and the fuel cost was reduced by 48%. [47] An optimization on solid waste collection and transport was performed by using the ArcGIS Network Analyst tool. As a result, a 48% gas saving was achieved on the optimal transport scenario. [48] Furthermore, a cooperative fuzzy optimization approach was utilized on the area of emergency transportation. Based on the approach, supplicated problems were break down to several sub-components and evaluated concurrently. The optimal solution was obtained by integrating all sub-solutions. By employing the approach, the decision making time can be reduced by 45 % to 83% for emergency transportation. [49] A multi-agent decision support system was created to perform transportation optimization with multiple requests and multiple routes. The objective of the optimization was minimizing the travel time and minimizing the gas emission. The optimal results regarding time and gas emission vary by the weight given to each criterion. [50].

1.7 Optimization Algorithm: MILP, GA

As the optimization algorithm, Mixed Integer Linear Programming (MILP) and Greedy Algorithm (GA) has been used broadly on mathematical models. In order to solve a EoL vehicle recovery problem in Turkey economically, a MILP optimization model was developed to minimize the costs on opening facilities, recovery processes, and transportation [51]. MILP was also applied on vehicle routing problems to maximize the on-time possibility with the shortest path. [52] In addition, MILP was utilized for optimizing the beam layout on multibeam satellite systems design. The result generated by MILP was excellent, but the computational speed can be further improved. [53]

Some advanced GA were developed on top of the original GA to solve specific problems. An iterated greedy algorithm was utilized for improving the current solution of permutation flowshop scheduling problems. With the algorithm, the final solution can be significantly improved by re-optimizing partial solutions. [54] A modified GA was employed to solve the stochastic control problem on the networked storage operation area. By deriving a sub-optimality bound to the algorithm, a semidefinite program can be constructed to minimize the bound. The algorithm is near-optimal because in many cases, the bound approaches zero. [55] A new, but generalized greedy: carousel greedy algorithm was developed to overcome weaknesses of the traditional greedy approaches. The new algorithm was used for solving several well-known combinatorial optimization problems. It showed that carousel greedy is able to handle problems with larger number of variables and can quickly generate a feasible solution. [56]

1.8 Aim and Contribution

The aim of the dissertation is to develop an optimal PV recycling framework by evaluating the amount of PV waste and to ensure the economic feasibility of the potential PV recycling infrastructure in California. Unlike previous studies, the main contribution is to include temporal and spatial consideration together for the PV recycling planning framework. Several mathematical models were constructed for determining the optimal locations PVRCs and generating the optimal distribution scenario. Sensitivity analysis was performed to test the efficacy the proposed mathematical model for facilitating decisions on building an efficient PV recycling network. The general framework allows efficient decision making for policymakers and stakeholders involved in PV recycling network.

CHAPTER II

METROLOGY

2.1 PV Recycling Framework Overview

A general framework was developed to facilitate PV recycling in local communities of the United States. Several mathematical optimization models were constructed to perform optimization. Figure 2.1 shows the overall structure of the PV recycling framework. First, a database was created for collecting input data on PV installation, various costs for PV recycling, distance matrices among PVIS, PVRC, and TC, and environmental impact index packages. The application of the database was shown in Chapter IV and Chapter VI. Second, for determining the optimal location of PVRC, multi-facility optimization model was developed and described in Chapter III. Third, for generating the optimal distribution scheme, optimal distribution model was developed and described in Chapter V. Case studies for multi-facility optimization model and optimal distribution model were demonstrated in Chapter IV and Chapter VI, respectively. Last, the framework can perform trade-off analyses between scenarios for guiding decision makings.

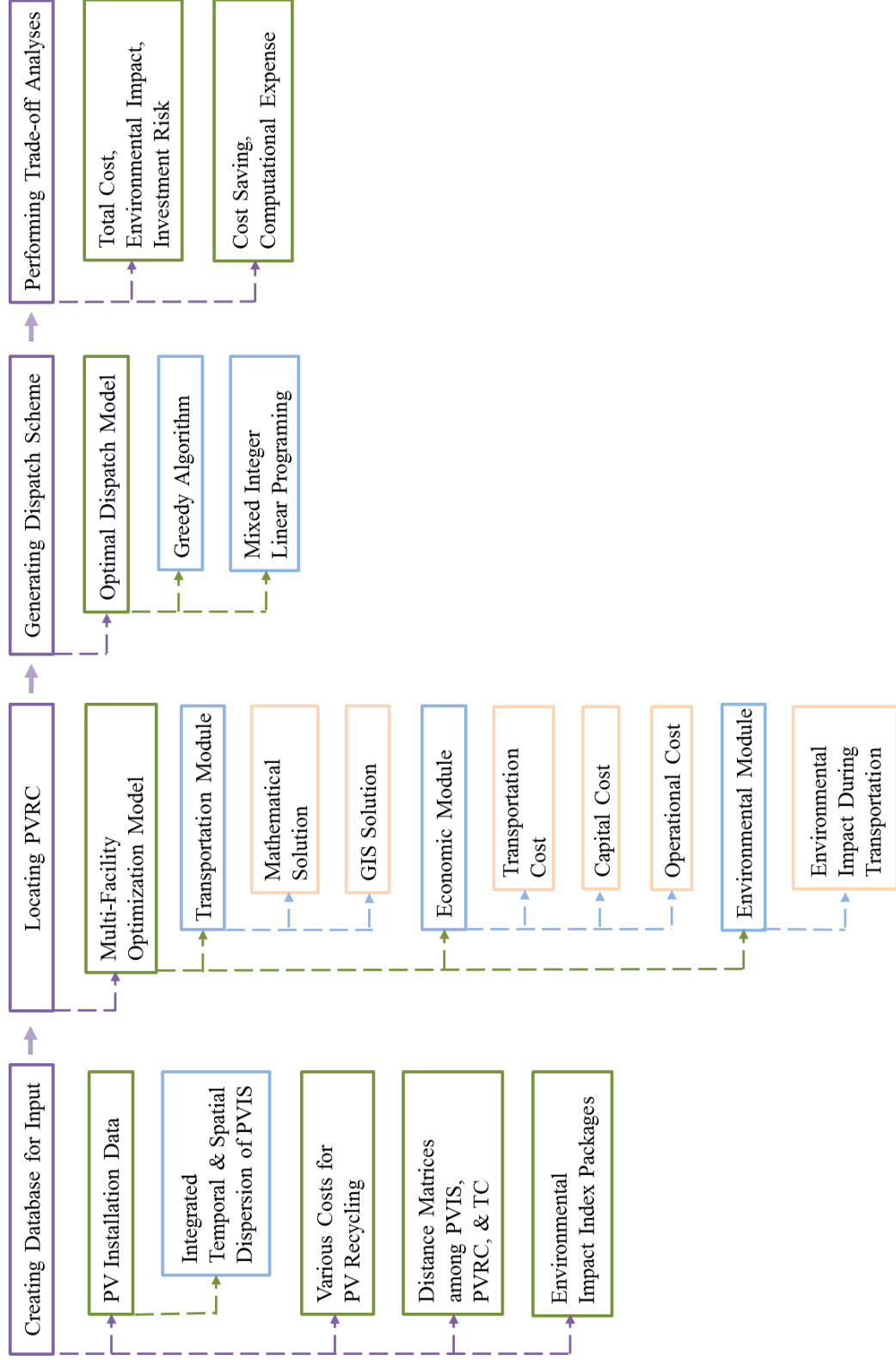


Figure 0.1: Structure of the PV recycling framework.

2.1.1 Creating Database for Input

The database consists of 1) PV installation data initiated by the U.S. National Renewable Energy Laboratory [14] under the U.S. Department of Energy; 2) various costs associated with setting up PV recycling center from real PV recycling industries; 3) distance matrices among PVIS, PVRC, and TC; 4) environmental impact index packages to evaluate the environmental impact of each recycling scenario.

2.1.2 Locating PVRC

The model should be able to generate multiple optimal scenarios varied by the number of PVRC and recycling periods. While optimizing, the model should be able to include realistic constraints such as the regional restrictions for building PVRCs and the annual recycling capacity of each PVRCs. In addition, the model should be able to handle the exponentially increased PV amount. Due to the exponentially increased amount of waste, several individual recycling periods, such as short, mid, and long terms should be considered separately. As the output, the model can give the geographical location of PVRCs, the total transportation distance, the break-down cost including the transportation cost, the capital cost, and the operational cost, and the environmental impact of each scenario in each recycling period.

2.1.3 Generating Distribution Scheme

From figure 1.1, the amount of PVIS varies a lot year by year. Thus, the optimization model should be smart enough for creating the distribution directives efficiently to satisfy the exponentially increased amount of PVIS. While performing the optimization process, the model should also be able to include the maximum annual capacity of each TC and

PVRC as physical constraints. As a result, an optimization model among three parameters: PVIS, TC, and PVRC needs to be constructed to distribution the most optimal TC to ship each PVIS to the closest PVRC.

2.1.4 Performing Trade-off Analyses

First, trade-off analyses should be performed among the total cost, the environmental impact, and the investment risk. Those three factors are affected by the location, the quantity, and the annual capacity of PVRC. Typically, lower total cost usually goes with higher environmental impact and investment risk. As a sustainable action, PV recycling is bringing tremendous environmental benefits on resource depletion and toxicity hazard. However, more positive effects are expected in the PV recycling process. As another sustainable manner, the environmental impact should be considered to make PV recycling much greener. In addition, as stakeholders, investment risk is much more interested than short-term investment profit. Therefore, multiple scenarios with trade-off analyses among cost, environmental impact and investment risk should be conducted for assisting the decision-making in PV recycling.

Second, while operating the distribution optimization among TC, PVIS, and PVRC, the first question should be addressed is whether the optimization process is necessary. It is not necessary to implement the optimization process if the total cost before and after the optimization are similar. Results from optimizations usually search for the global minima, but could be significantly time consuming. Thus, Sensitivity analyses should be performed among scenarios to explore the necessity of the optimization process. General recommendations should be concluded for directing the optimization in the necessity perspective on PV recycling.

2.2 Uniqueness of the proposed work

2.2.1 Integration of Temporal and Spatial Dispersion of PVIS

This research integrated multiple dimensions of data into one model while developing the PV recycling framework. In the multi-facility optimization model, the geographical variance and time variance of PVIS was considered as a whole. In the geographical variance perspective, for addressing the uneven dispersion of PVIS, a mathematical optimization model was developed to select the location of PVRCs. While addressing the exponential increase of PVIS year by year (the time variance issue), the research creatively proposed three recycling phases to construct PVRCs periodically.

2.2.2 Development of Multi-Facility Optimization Model

Multi-facility optimization model considered the interplay among return of investment, environmental impact, and investment risk while planning PV recycling. Trade-off analyses were performed among those factors by considering several uncertain situations. Consequently, several recycling scenarios were concluded.

2.2.3 Development Optimal Distribution Model

Optimal distribution model was developed to generate the transportation schemes between PVIS, PVRC, and TC. Two creative algorithms: static and dynamic computational algorithm was employed to construct the model for conducting the optimal distribution scenario. Besides the computational results, the research also focused on the performance of two algorithms from the cost-effectiveness perspective. The practicability of each algorithm was discussed.

2.2.4 Utilization of GIS for PV Recycling Optimization

As an alternate way to solve the location allocation problem, GIS was utilized to find the optimal location of PVRC. The median center and the spatial join were used as the optimization tool. The location and the distance results concluded by the multi-facility optimization model and GIS were compared. In addition, GIS was also used for displaying the spatial and the temporal dispersion of PVIS and the locations of PVRC in scenarios.

CHAPTER III

MULTI-FACILITY OPTIMIZATION MODEL

A general mathematical modeling framework is developed to optimize the economic and environmental performance of the PV reverse logistics network. There are three aspects in the proposed model: 1) transportation module; 2) economic module; 3) environmental module.

3.1 Transportation Module

The transportation module locates Photovoltaic Recycling Centers (PVRCs) in the optimal geographical regions by minimizing the total travel distance (TTD) for the collection of retired PV modules from PV Installation Sites (PVIS) to PVRCs. In the transportation module, the geographical location, and the installed year of PVIS were required as the input. Those spatial and temporal information can be achieved from various publicly available sources [57, 58]. As a result, a mathematical model was developed for selecting optimal locations of PVRCs by minimizing the total transportation distances. The weight of the material of each PVIS and the capacity of PVRC were considered in the module.

3.1.1 Distance Definition

On a two-dimensional surface, the geometric distance between two locations (x_1, y_1) and (x_2, y_2) can be defined as [39] :

$$D^s = \sqrt{(x_1 - x_2)^2 + (y_1 - y_2)^2} \quad (3.1)$$

Therefore, the geometric distance of two longitude and latitude based locations $(\text{long}_1, \text{lat}_1)$ and $(\text{long}_2, \text{lat}_2)$ on a flat two-dimensional surface is:

$$D^l = \sqrt{(\text{long}_1 - \text{long}_2)^2 + (\text{lat}_1 - \text{lat}_2)^2} \quad (3.2)$$

However, in practice, on earth, the distance between two longitude and latitude based locations, instead of the linear distance, should be modified to the arc distance, in which,

The length of 1° of longitude

$$\begin{aligned} &= \cos(\text{latitude}) \times \text{length of degree (miles) at equator} \\ &= \cos(\text{latitude}) \times 69.172 \text{ miles} \end{aligned} \quad (3.3)$$

$$\text{The length of 1° of latitude} = 1^\circ \times 69.172 \text{ miles} = 69.172 \text{ miles} \quad (3.4)$$

Thus, the arc distance on earth can be expressed as equation 3.5 with the unit of the distance of the formula is expressed in miles [59]. Equation 3.5 was use as a distance calculating equation and was denoted by method 1.

$$D^{(1)} = \sqrt{[(\text{long}_1 - \text{long}_2) \times c \times \cos(\text{lat}_1 - \text{lat}_2)]^2 + [(\text{lat}_1 - \text{lat}_2) \times c]^2} \quad (3.5)$$

where, longitude and latitude are both measured in degrees (decimal), and c ($c = 69.172 \text{ miles/degrees}$) converts the units from degrees to miles.

In addition, by considering approximate sphere shape of earth, the distance between two points on earth can also be calculated as the spherical distance [60] in equation 3.6. Equation 3.6 was use as another distance calculating equation and was denoted by method

2. The distance calculated by both methods were compared for achieving the global minimum.

$$D^{(2)} = 2 \times R \times \sin^{-1} \left(\sqrt{\sin^2 \frac{lat_1 - lat_2}{2} + \cos lat_1 \times \cos lat_2 \times \sin^2 \frac{long_1 - long_2}{2}} \right) \quad (3.6)$$

where, R is the radius of earth and equals 3,959 miles. $D^{(2)}$ is the arc-length distance on earth.

3.1.2 Distance in PV Recycling

The optimal quantity, and locations of PVRC needs to be determined. For the centralized scenario, which has a single PVRC, all EoL PV are brought into that PVRC. Thus, the only task is to find the location of the center in order to minimize the total travel distance. For decentralized scenarios, where the number of PVRC varies from two to ten, the optimization process is more challenging: the selected PVRC should be the one that has the smallest distance between the PVIS and the PVRC, also not exceeding its maximum annual capacity.

In addition, while determining the location of PVRC, the weight of material of each PVIS should be considered because intuitively, PVRC should be closed to large PVIS than small PVIS. So the distance calculating equation 3.5 and 3.6 can be modified as equation 3.7 and 3.8, respectively.

$$D^{(1w)} = \sqrt{[(long_1 - long_2) \times c \times \cos(lat_1 - lat_2)]^2 + [(lat_1 - lat_2) \times c]^2} \times W \quad (3.7)$$

$$D^{(2w)} = R \times \sin^{-1} \left(\sqrt{\sin^2 \frac{lat_1 - lat_2}{2} + \cos lat_1 \times \cos lat_2 \times \sin^2 \frac{long_1 - long_2}{2}} \right) \times W \quad (3.8)$$

where, W is the weight of material of each PVIS.

If all location of PVIS are denoted as (a_i, b_i) and all locations of PVRC are denoted as (x_j, y_j) , equation 3.7 and 3.8 can be expressed as 3.9 and 3.10, respectively. All (a_i, b_i) are known and all (x_j, y_j) are unknown.

$$D_{i,j}^{(1w)} = \sqrt{[(a_i - x_j) \times c \times \cos(b_i - y_j)]^2 + [(b_i - y_j) \times c]^2} \times W_i \quad (3.9)$$

$$D_{i,j}^{(2w)} = 2 \times R \times \sin^{-1} \left(\sqrt{\sin^2 \frac{b_i - y_j}{2} + \cos b_i \times \cos y_j \times \sin^2 \frac{a_i - x_j}{2}} \right) \times W_i \quad (3.10)$$

If multiple locations of PRRC are included in the scenario, the weighted distance between the PVIS i and the selected PVRC j to recycle the PVIS i is

$$D_i^{(w)} = \min D_{i,j}^{(w)} \quad (3.11)$$

where $D_{i,j}^{(w)}$ can be either $D_{i,j}^{(1w)}$ or $D_{i,j}^{(2w)}$ depending on whichever distance calculating method is used.

The total weighted distance to recycle all PVIS is in equation 3.12, which is also the objective function of the optimization.

$$D^{(w)} = \sum_{i=1}^n D_i^{(w)} \quad (3.12)$$

After the locations of PVRC are calculated as (x'_j, y'_j) by the optimization process, the distance between the PVIS i and the selected PVRC j to recycle the PVIS i is

$$D_{i,j}^{(1)} = \sqrt{[(a_i - x'_j) \times c \times \cos(b_i - y'_j)]^2 + [(b_i - y'_j) \times c]^2} \quad (3.13)$$

$$D_{i,j}^{(2)} = 2 \times R \times \sin^{-1} \left(\sqrt{\sin^2 \frac{b_i - y'_j}{2} + \cos b_i \times \cos y'_j \times \sin^2 \frac{a_i - x'_j}{2}} \right) \quad (3.14)$$

The distance between the PVIS i and the selected PVRC j to recycle the PVIS i is

$$D_i = \min D_{i,j} \quad (3.15)$$

where $D_{i,j}$ can be either $D_{i,j}^{(1w)}$ or $D_{i,j}^{(2w)}$ depending on whichever distance calculating method is used.

The total transportation distance is

$$D = \sum_{i=1}^n D_i \quad (3.16)$$

In order to illustrate the optimization mechanism, the 3-PVRC case is shown as an example to recycle the 1st PVIS by using method 1 in equation 3.5. The longitude and latitude of the 1st PVIS is (a_1, b_1) , and (x_1, y_1) , (x_2, y_2) , and (x_3, y_3) for the three PVRC. The weighted distances between the 1st PVIS and PVRC are

$$D_{1,1}^{(1w)} = \sqrt{[(a_1 - x_1) \times c \times \cos(b_1 - y_1)]^2 + [(b_1 - y_1) \times c]^2} \times W_1 \quad (3.17)$$

$$D_{1,2}^{(1w)} = \sqrt{[(a_1 - x_2) \times c \times \cos(b_1 - y_2)]^2 + [(b_1 - y_2) \times c]^2} \times W_1 \quad (3.18)$$

$$D_{1,3}^{(1w)} = \sqrt{[(a_1 - x_3) \times c \times \cos(b_1 - y_3)]^2 + [(b_1 - y_3) \times c]^2} \times W_1 \quad (3.19)$$

The travel distance between the 1st PVIS and the selected PVRC $D_1^{(1w)}$ is the minimum distance among above three:

$$D_1^{(1w)} = \min(D_{1,1}^{(1w)}, D_{1,2}^{(1w)}, D_{1,3}^{(1w)}) \quad (3.20)$$

For the 3-PVRC scenario, the objective function in the optimization process is

$$D^{(1w)} = \sum_{i=1}^n D_i^{(1w)} \quad (3.21)$$

The optimal location of those three PVRC can be determined by the optimization process. The locations are (x'_1, y'_1) , (x'_2, y'_2) , and (x'_3, y'_3) . The distances between the 1st PVIS and those three PVRC j are

$$D_{1,1}^{(1)} = \sqrt{[(a_1 - x'_1) \times c \times \cos(b_1 - y_1)]^2 + [(b_1 - y'_1) \times c]^2} \quad (3.22)$$

$$D_{1,2}^{(1)} = \sqrt{[(a_1 - x'_2) \times c \times \cos(b_1 - y_2)]^2 + [(b_1 - y'_2) \times c]^2} \quad (3.23)$$

$$D_{1,3}^{(1)} = \sqrt{[(a_1 - x'_3) \times c \times \cos(b_1 - y_3)]^2 + [(b_1 - y'_3) \times c]^2} \quad (3.24)$$

The travel distance to recycle the 1st PVIS is the minimum distance among those three distances:

$$D_1^{(1)} = \min(D_{1,1}^{(1)}, D_{1,2}^{(1)}, D_{1,3}^{(1)}) \quad (3.25)$$

The total transportation distance for recycling all PVIS in the 3-PVRC scenario by using method 1 is

$$D^{(1)} = \sum_{i=1}^n D_i^{(1)} \quad (3.26)$$

3.1.3 Optimization Tool

As part of the optimization processes, “fmincon” function in Matlab [61] was employed to determine the latitude and the longitude of PVRC. Fmincon function is one of built-in functions in Matlab. The function can be used to find the minimum solution for either linear and nonlinear functions subjected to given constraints. For initiating the optimization, users need to compile an objective function, upload input data, define the initial guess. Several constraints and the upper and lower bounds can be included into the function if needed. By calling the function, the minimum value of the function, as well as its solved unknowns can be produced. The expression of the function is shown below:

Minimize

$$f(x) \tag{3.27}$$

Subject to

$$c(x) \leq 0 \tag{3.28}$$

$$c_{eq}(x) = 0 \tag{3.29}$$

$$A \cdot x \leq b \tag{3.30}$$

$$A_{eq} \cdot x = b_{eq} \tag{3.31}$$

$$lb \leq x \leq ub \tag{2.32}$$

where, $f(x)$ is the objective function that needs to be minimized. x is the variable which can be a scalar, vector, or matrix. The return of the function is a scalar. The constraints in equation 3.28 and 3.29 are nonlinear inequalities and nonlinear equalities, respectively. $c(x)$ and $c_{eq}(x)$ are functions that return vectors. The constraints in equation 3.30 and 3.31 are linear inequalities and linear equalities, respectively. A and A_{eq} are matrices and x , b , and b_{eq} are vectors. The constraint in equation 3.32 is the lower and upper bound of the variable x . The lower bound (lb) and the upper bound (ub) can be defined as a vector or a matrix according to the dimension of x .

In the PV recycling optimization, the objective function is a nonlinear function because it contains the square and the square root operators. It is also a discrete function because of containing the logical operator “min”. The input consists of the latitude, the longitude, the weight of material of each PVIS. The initial guess was defined as a $n \times 2$ matrix, in which n is the number of PVRC and 2 represents the longitude and latitude of each PVRC. The

upper and the lower bound were set according to the geographical bound of California, which were set as (-125, -114) and (32, 42) for longitude respectively.

3.1.4 Mathematical Model

Based on the mechanism of fmincon function, we have adopted a mathematical model which optimizes the locations of multiple recycling facilities. Equation 3.33 is the objective function which minimizes the total distance travelled for delivering the retired EoL PV modules from multiple PVISs to multiple PVRCs. Equation 3.34 ensures all retired PV modules from each PVIS are delivered to the closest PVRC. The linear inequalities in the Equation 3.35 restrict that the total weight that each PV PVRC receives is less than its maximum accepted capacity. The annual capacity of each PVRCs for different case needs to be specified to run the model. In order to ensure the feasibility of the mathematical model, maximum capacity of each PVRC set to be greater than the total amount of incoming PV modules delivered to each PVRC. The model is designed to send any excess amount of incoming PV modules to the next available PVRCs if it reaches the maximum capacity. Equations 3.36 and 3.37 sets geographical boundaries of the considered regions. The model iterates until the optimal locations of PVRCs are found.

Minimize

$$F(\Phi, \Lambda) = \sum_{i=1}^n \sum_{j=1}^n D_{ij} \cdot X_{ij} \cdot W_i \quad (3.33)$$

Subject to

$$\sum_{j \in J} X_{ij} = 1 \quad (3.34)$$

$$\sum_{i \in I} W_i X_{ij} \leq C_j \quad (3.35)$$

$$lb_\phi \leq \phi_j \leq ub_\phi \text{ for all } \phi_j \text{ in } \Phi \quad (3.36)$$

$$lb_\lambda \leq \lambda_j \leq ub_\lambda \text{ for all } \lambda_j \text{ in } \Lambda \quad (3.37)$$

The main outcomes of the model are the optimal geographical location of PVRC and the total transportation distance. Total distance traveled can be calculated by summing up all optimized distance from each PVIS to the designated PVRC as shown in equation 3.38.

$$D(\Phi, \Lambda) = \sum_{i=1}^n \min(D_{ij}) \cdot n_i \quad (3.38)$$

where, $\min(D_{ij})$ is the shortest distance between each PVIS i and corresponding PVRCs j . n_i represents the number of trips required. After the transportation module determines the total distance traveled for each scenario, economic and environmental impacts can be accounted in the following modules.

3.1.5 Local and Global Minimum

A local minimum is the smallest value of the function within a sufficiently small neighborhood about the minimum point, whereas the global minimum is the smallest value over the entire domain of a function. Thus, the global minimum of the function is also one of local minima, and the global minimum of that function is always the smallest local minimum. Also, the global minimum may not exist for unbounded functions. [62] Figure 3.1 represents the relationship of the local minimum and the global minimum.

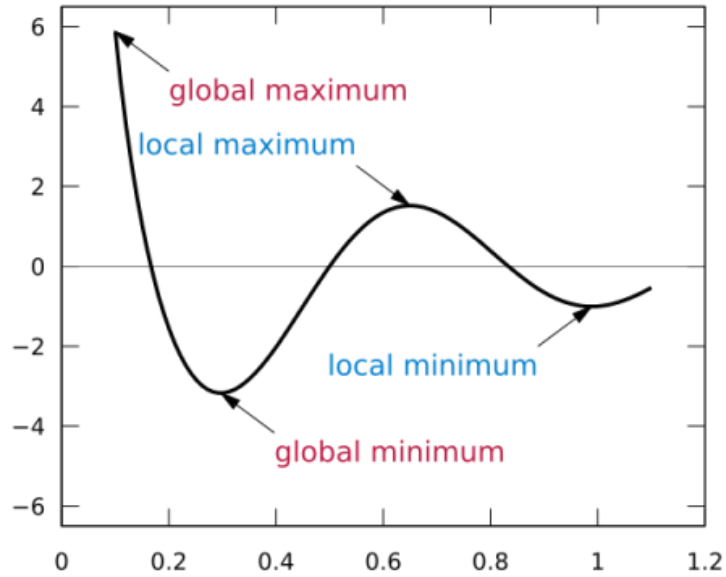


Figure 0.1: Demonstration of local minimum and global minimum.

The local minimum issue may arise in situations while the objective function is in nonconvex or discrete situation. In general, while finding the minimum, algorithms converge to a minimum, but that minimum might be a local minimum. Initial guesses affect the iteration stopping at a local minimum or the global minimum. Thus, appropriately selecting initial guesses is a key factor to finding the global minimum on the nonconvex, discrete, nonlinear, and multiple variable functions. Multiple start points are usually used in order to obtain the global minimum.

In the PV recycling problem, while locating PVRC, the objective function is discrete and nonlinear. The reason of that is the existence of the logic and square root operators. Furthermore, as the number of the recycling centers increases from two to ten, the objective function turns out to be multivariable and nonconvex. The global minimum does exist because the objective function subjects to a closed interval, which is in the geographical

bounds of the state of California. However, it is challenging to obtain the global minimum among all local minima. The following actions were applied to facilitate obtaining the global minimum.

- **Apply multiple initial guesses and several Optimization algorithms**

In order to determine the global minimum, multiple initial guesses and several optimization algorithms were applied in the optimization process [63]. First, several starting values were used including several values such as (1, 1) and (-120, 35). Also, the results obtained from the last or the next scenario were used as initial guesses. Second, the fmincon solver has several optimization algorithms such as active-set, sqp, interior-point, and trust-region-reflective build in. The combinatorial initial guesses and algorithms were used for repetitive trials and the smallest local minimum was picked as a potential global minimum.

- **Use two different distance calculating methods**

In addition, two different distance calculating methods were applied while performing the optimization. The total transportation distance conducted by two methods were plotted and compared. The smaller value in each scenario tends to be the global minimum and was picked. In addition, with the number of PVRC increases, the slope of the total travel distance should decrease gradually. If any increase, shock, or fluctuation occurs at any point on the plot, the global minimum of that scenario has not been reached yet.

- **Plot PVRC location on maps**

After finding the geographical location of each recycling center, ArcGIS was utilized to visually present all locations of each scenario on the California. Intuitively, in order to minimize the total travel distance, all locations of recycling centers should be close to PV

installing clusters. Besides, scenarios next to each other should have similar locations of PVRC. One additional PVRC added based on the previous scenario. If any one of two criteria are not satisfied, the global minimum has not been researched yet. The local minimum issue can be easily detected by presenting the location results on the map via ArcGIS.

3.1.6 Alternate Optimization Tool: GIS

As an alternate way, GIS can be used to find the optimal location of PVRC as well as the total transportation distance. The median center tool and the spatial join tool can be used as the optimization tools. The median center tool in ArcMap can be used to find the geographical locations of PVRC. Median center in ArcMap is the location that minimizes overall Euclidean distance among all elements of a dataset. The tool also considered the weight of material of each PVIS while locating median centers. Consequently, all PVRCs can be located closer to large PVISs: the larger the PVIS is, the closer the PVRC is nearby. After obtaining the location of PVRCs, the total transportation distance can be calculated by using the spatial join tool. Spatial join is a tool that mates each PVIS to the closest PVRC. The total transportation distance can be obtained by summing all individual distances together.

For doing the optimization, employing GIS of requires less programming work than applying the mathematical models described in 2.1.2 and 2.1.3. The location of PVRC and the total transportation cost can be simply obtained after the location and the weighted of material of PVIS are uploaded into GIS. As the disadvantage, GIS can only find one median center in each research area. In order to obtaining multiple locations of PVRC in multiple PVRC scenarios, the research area needs to be physically divided to the corresponding

number of areas. The result of the GIS method is not expected to be as accurate as the method by using mathematics and programming as human subjects are included while dividing research areas. However, the method is still worth to try if the result is not way off from the programming method.

3.2 Economic Module

The economic module evaluates the recycling system's economic performance. Overall PV recycling cost consists of 1) transportation costs, 2) capital costs, and 3) operating costs. After the optimal locations of PVRCs are decided from the transportation module, transportation costs can be calculated based on the total transportation distance travelled. Evaluation of the total transportation cost requires inputs such as the maximum capacity and fuel efficiency of trucks, fuel prices of different geographical locations, costs for truck drivers/contracting service. Following assumptions are made for the modeling: maximum load of lorry is 7.5 metric tons; fuel efficiency of truck is 3.85 km/L; cost of fuel is \$0.99/liter; hourly wage of truck driver in the state of California is \$25/hr; approximate weight of the 1MW capacity PV modules are equivalent to 75 metric tons [32]. The capital cost includes the cost on plant, equipment, and land. The operating cost includes the costs of labor, utility, and maintenance. Some indirect cost such as administrative cost should be included as well. Evaluation of total costs requires inputs such as the annual optimal recycling capacity and annual operating costs of each PVRC are chosen from the transportation module. We have adopted functional relations among the capital cost, operating cost, and the annual capacity from a model developed by a study [64]. The cost models include the economies of scale when considering the cost variants related to the size of the PVRC capacity.

3.3 Environmental Module

The environmental module assesses the environmental impact of the PV recycling generated from transportation scenarios. Global Warming Potential (GWP) impact is used as the main indicator to account the lifecycle environmental impacts generated from transportation. Greenhouse gas inventories from Ecoinvent V. 2.1 [65] for the operation stage of the truck is utilized. Direct airborne emissions of gaseous substances, particulate matter, and heavy metals are accounted for. Average environmental data for 50 percent loaded heavy-duty vehicles are assumed as a conservative measure. Emission from trucking assumed to be linear with the transportation distance. GWP over 20 years (GWP20) are used [66]. Other environmental impacts can be calculated readily but we presented GWP only in this study.

CHAPTER IV

CASE STUDY OF MULTI-FACILITY OPTIMIZATION MODEL

The proposed framework in chapter IV was applied to the California because the state has relatively long history and a larger size of PV installations compared to other states. The overall framework considers the variances of temporal and spatial parameters vis-à-vis for short, middle, and long term planning.

4.1 PV Installation Size, Type, and Location

Main data used for the modeling include such as the location of the PV installation, the size, and the year of installation of 53,846 PV sites. Based on these data, we have classified three different time periods of PV installation in California. Figure 4.1 shows the PV installation in California from 1984 to 2015. In the first period (i.e. Introduction of PV during 1984-2005), PV modules were installed in a small scale, mostly as residential systems of relatively slow growth rate. In the second period (i.e. Fast Growth of the PV market in CA during 2005-2010), PV installation picked up relatively fast because of the establishment of incentive policies in California. In 2005, the California Solar Initiative (CSI) was approved by the California Public Utilities Commission (CPUC) for providing subsidies on solar projects. A \$2 billion budget over 10 years was proposed by CSI. In

2006, more than \$3 billion were provided by CSI as incentives on small PV systems throughout residential, commercial, governmental and nonprofit buildings [67]. In the third period, (i.e., large-scale), lot more utility scale PV modules have installed in various locations in CA. However, there was a sudden drop of the installation capacity in the year 2013 partly because of the winding down of CSI; the subsidy of installing PV is reduced significantly from \$2.50 to \$0.20 per watt [68]. In addition, CPUC changed the electricity rate structure from four-tier to three- or two tier in 2013 [69].

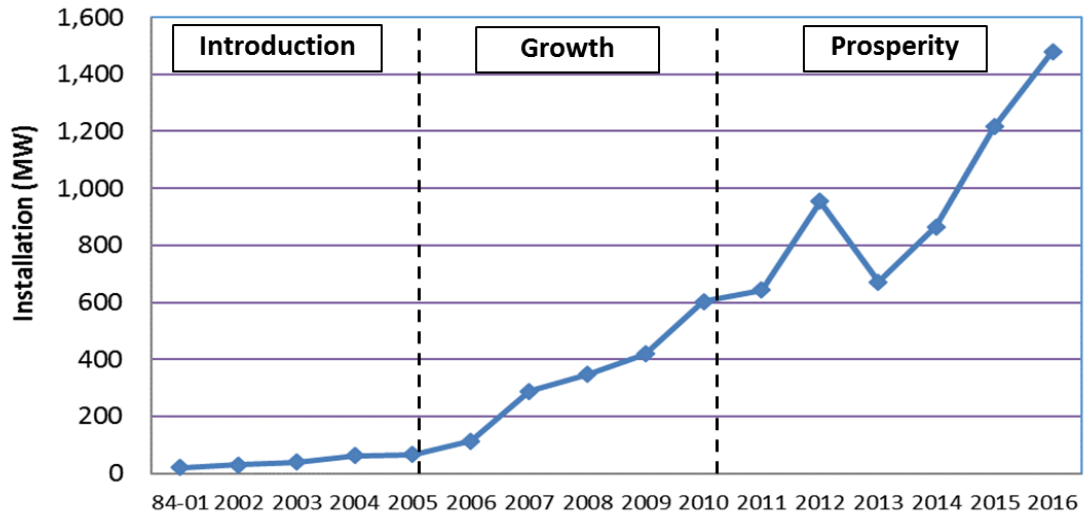


Figure 0.1: Annual PV installations in California (1984 – 2016).

Table 4.1 lists the variation in size and the number of PVISs locations in the three periods of PV installation [57, 58]. The total number of new PVIS constructed are 2,706, 14,875 and 36,265 for introduction, growth, and prosperity periods, respectively. We couldn't include data for the 2016 as it is not available in the source. In the growth and prosperity periods, total size of new installation is an order of magnitude larger than those

of the introduction period. Basically, it shows that small residential PV installation dominates compare to the large utility scale installation in terms of the number of PVIS. However, in terms of the capacity of PVIS, utility scale installation is an order of magnitude larger than total small scale residential installation.

Table 0.1: Number of sites and size of PVIS.

Capacity of PVIS (kW)	Introduction			Growth			Prosperity		
	# of Sites	%	Size (MW)	%	# of Sites	Size (MW)	%	# of Sites	Size (MW)
up to 3	15,093	46%	34	16%	32,472	71	4%	77,366	173
~ 5	7,015	21%	27	13%	41,961	165	9%	152,138	613
~ 7	5,433	17%	32	15%	28,511	169	10%	118,201	701
~ 10	2,464	8%	21	10%	17,126	141	8%	75,899	623
~ 25,000	2,691	8%	102	47%	14,793	1,222	69%	35,605	2,240
Total	32,696	100%	216	100%	134,863	1,768	100%	459,209	4,350

Figure 4.2 shows more visual insights about PV module installed during the year 1984 to the year 2015 in different locations of California. Horizontal axis is the number of PVIS and vertical axis shows the capacity installed. Each dot indicates the size of the PV installed. For example, first dot in the far left side of the x-axis indicates the 1,133 kW installed in one area of CA (Dot 1), and the next dot below indicates the 908 kW system installed in the other area of CA (Dot 2). Each color indicates the year of installation and the triangular dots indicate the installation capacity over 1.2 MW system. It shows the relationship among the size, year of installation, and number of installed sites. For example, the width of the regions (i.e. aggregated dots) in year 2014 is wider than year 2012 (i.e. more PVIS). However, the total installed capacity in the year 2012 was higher than that of the year 2014 (i.e. figure 4.1). It is obvious that there were larger scale PVIS (triangular dots) in the year 2012 than the year 2014. In terms of the number of PVIS, small scale systems such as less than 3 kW and 10 kW cover twenty and ninety percent of the total accumulative installation in CA respectively. In addition, large scale installation (i.e. more than 1.2 MW) counts less than one percent in terms of the number of sites but covers seven percent in terms of the total capacity.

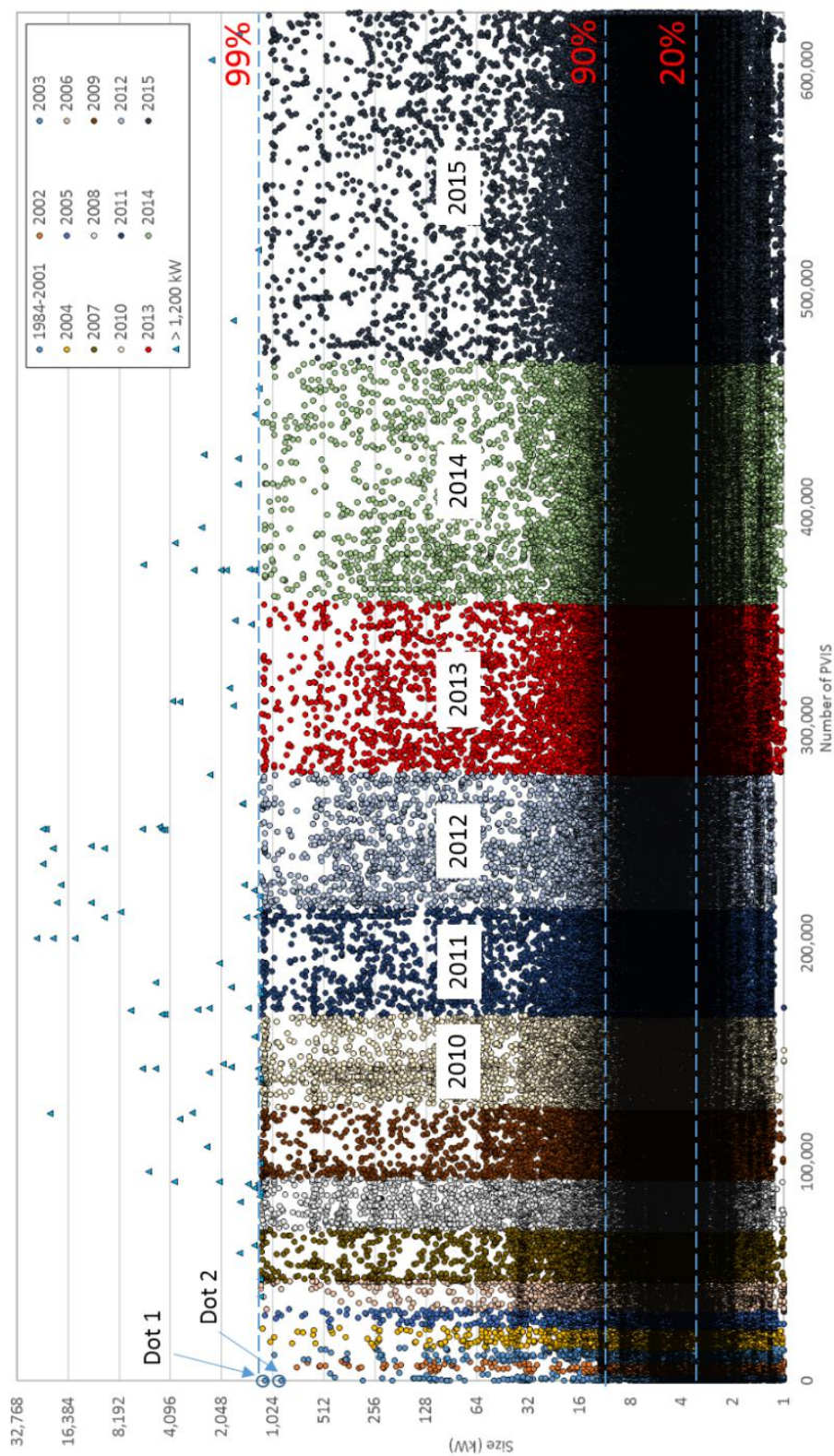


Figure 0.2: Size of the installed PV during 1984 - 2015 in CA.

4.2 Phase I: Short-term Planning

This section shows the case of selecting optimal numbers and locations of PVRCs in CA to process EOL PV modules expected to retire during 2021 ~ 2025 (i.e. modules installed in introductory period). Based on the waste prognosis, initial recycling facilities capable of processing a total of 70 MW per year PV EOL waste is suggested. Table 4.2 shows the annual capacity of each PVRC, the total transportation distance (TTD) from PVIS to the optimal PVRC location, the breakdown of the cost, and corresponding CO₂ emissions from transportation as the number of PVRC increases. TTD decreases as the number of PVRCs increase since the model allocate smaller size of PVRCs to more decentralized locations to process annual total waste 70MW. For example, adding second PVRC can result in 63 percent reduction of TTD compare to single PVRC case. Adding third PVRC only reduces additional 5 percent of TTD compare to 1 PVRC case. It is modeled that the waste which could not be processed because of the capacity limit of the plant will be put on hold in inventory to be processed next year/phase in the same PVRC.

Table 0.2: Total costs and emission generated from the Phase I planning.

Number of PVRC	Capacity (mT/year/PVRC)	TTD (10 ⁶ km)	Capital (\$M)	O&M (\$M)	Transport (\$M)	Total Cost (\$M)	GWP (10 ³ ton-CO ₂ eq)
1	5,300	9.5	0.7	2.2	5.9	8.8	1,390
2	2,600	3.5	0.9	2.9	2.5	6.3	513
3	1,800	3.0	1.1	3.4	2.2	6.6	444
4	1,300	2.6	1.2	3.7	1.9	6.9	376
5	1,100	2.1	1.3	4.0	1.7	7.0	314
6	900	1.9	1.4	4.3	1.5	7.2	275
7	800	1.7	1.5	4.4	1.4	7.3	249
8	700	1.5	1.6	4.6	1.3	7.5	228
9	600	1.5	1.6	4.7	1.3	7.6	215
10	500	1.4	1.7	4.9	1.2	7.8	200

Figure 4.3 shows the trend of the total system costs as the number of PVRCs increases. This result stems from the relative relationship between the transportation cost savings (i.e. distance savings) and the other costs associated with setting and operating PVRCs with different capacity (i.e. as the number of PVRC increase, the capacity of PVRC decrease) to process total 70MW of PV waste in this period in CA. Total system capital cost and the operation cost increases, while the transportation cost decreases as the number of the constructed PVRCs increase.

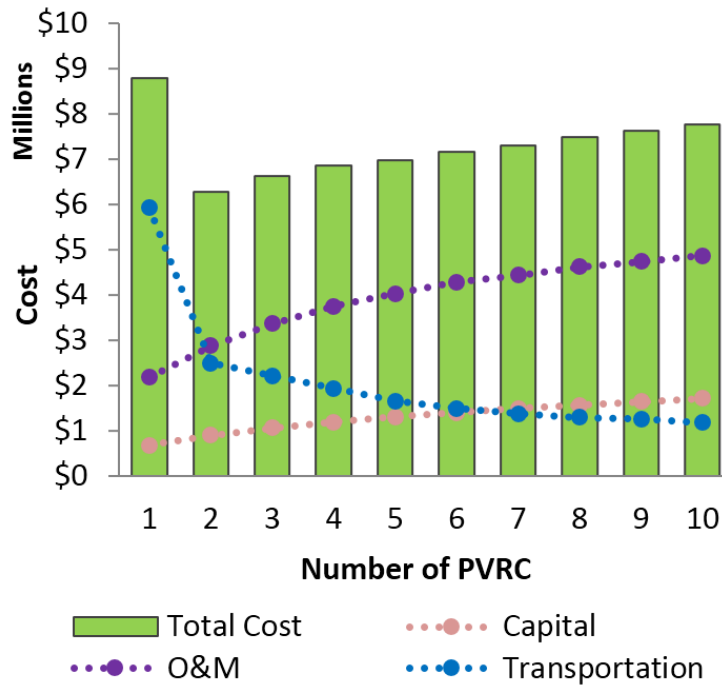


Figure 0.3: Total system cost vs. number of PVRC in Phase I.

Optimal numbers and locations can be selected based on the size of PV waste generated, TTD, capacity limit of PVRC, and recycling costs. Our goal is to show diverse options for decision makers when they plan for constructing PVRC for processing the PV waste generated from the installation during the “introduction period” (1984-2005). To

show the efficacy of the model, we have selected constructing two 35 MW processing capacity (i.e. total 2,600 tonne PV waste processing per year) PVRCs in the two optimized locations since the scenario seems to provide the best return on investments with the least environmental impacts as shown in Table 3.2. Figure 4.4 shows the geographical location of different size of PVIS installed in the introduction period. It also shows the latitude and longitude of selected optimal PVRC locations. Other numbers of PVRC map can be found in appendix A-1.

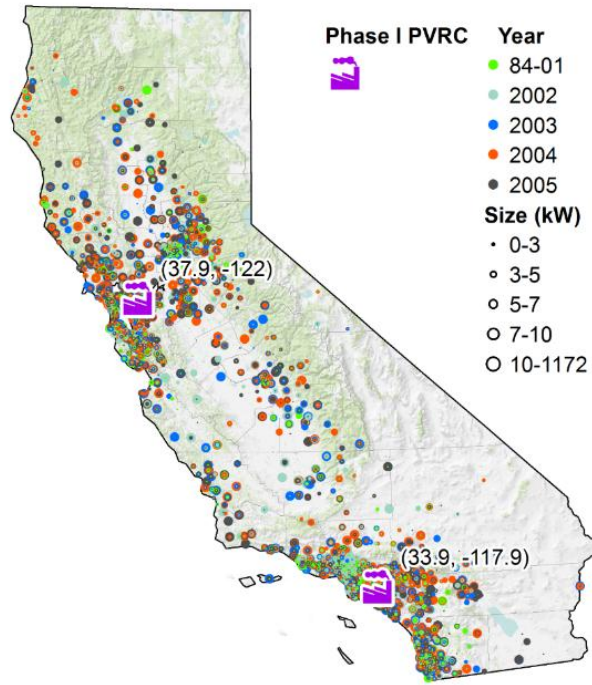


Figure 0.4: Two PVRCs selected for Phase I (2021 - 2025).

4.3 Phase II: Mid-term Planning

This section shows the case of selecting optimal numbers and locations of PVRCs in CA to process EOL PV modules expected to retire during 2026 ~ 2030 (i.e. modules

installed in the Growth period). Based on the waste prognosis, recycling facilities capable of processing total 700 MW per year PV EOL waste is suggested. Since, two smaller scale PVRCs are already constructed from Phase I to process total 70 MW of PV wastes, new PVRCs which can process additional 630 MW (i.e 47,000 tonne) of EOL PV waste per year are required. Optimal numbers and locations of new additional PVRC (different capacities than PVRC in Phase I) are selected based on the size of PV waste generated in the Growth period, TTD, capacity limit of PVRC, and the recycling costs. Table 4.3 shows TTD from PVIS to the optimal PVRC locations, corresponding recycling costs, and the associated environmental impacts. Decentralized scenarios can disperse the financial risk of the entire reverse logistics network planning. If the profitability was not quite well in the future, some PVRC can be closed with relatively less financial risk. Second, operation costs (especially labor costs) take up about 60 percent in Phase II planning. Development of new recycling technologies with more automations and advanced processes can reduce the labor costs significantly.

Table 0.3: Total costs and emission generated from the Phase II planning.

# of new PVRC	Capacity (mT/year /PVRC)	TTD (10 ⁶ km)	Capital (\$M)	O&M (\$M)	Transport (\$M)	Total Cost (\$M)	GWP (10 ³ ton-CO ₂ eq)
3	16,000	10.8	4.0	11.0	7.6	22.5	1,584
4	12,000	9.0	4.4	12.2	6.5	23.2	1,330
6	8,000	7.4	5.2	14.2	5.4	24.8	1,057
8	6,000	7.2	5.9	15.3	4.7	25.8	874

Figure 4.5 shows the trend of the total system cost when additional PVRCs are added in Phase II. As in Phase I, TTD decreases as the number of PVRCs increase since the model allocated smaller PVRCs to more decentralized locations to process an annual total waste

of 700 MW. In purely monetary terms, constructing two additional PVRCs seems providing the best economic return. However, if only two additional PVRCs are constructed, the size (i.e. annual capacity) of those two additional PVRCs would be almost ten times larger (i.e. 315 MW each – 24,000 tonne) than the two existing PVRCs selected in phase I.

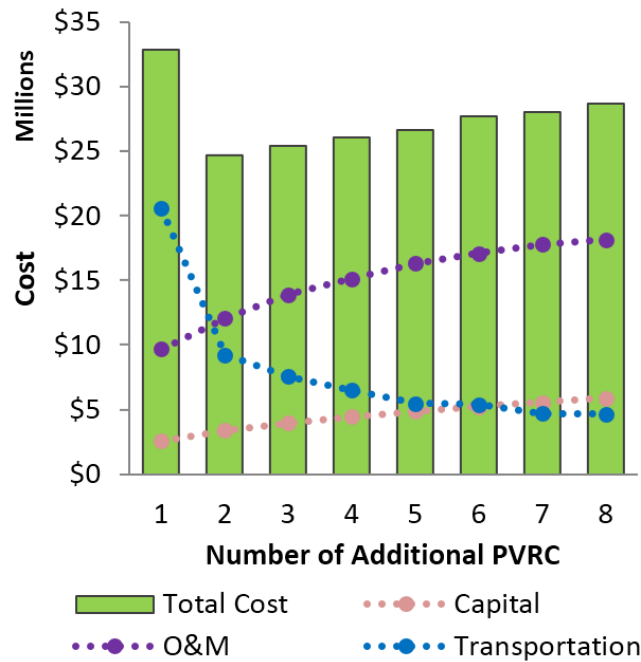


Figure 0.5: Total system cost vs. number of additional PVRCs in Phase II

It is still decision maker's discretion for selecting additional number of PVRCs in Phase II. However, we took a conservative approach and picked allocating six additional PVRCs in the optimal decentralized location (i.e. additional 8,000 tonne per year processing capacity per PVRC) in this phase. Figure 4.6 shows the geographical location of different size of PVIS installed in the growth periods. It also shows the latitude and longitude of two

PVRCs constructed in Phase I and six new PVRCs constructed in Phase II. Other numbers of PVRC map can be found in appendix A-2.

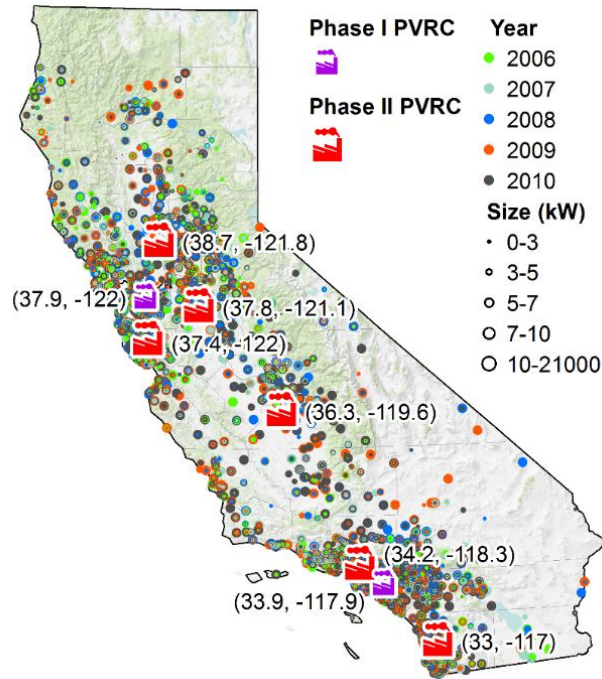


Figure 0.6: Six PVRC selected for Phase II (2026 - 2030).

4.4 Phase III: Long-term Planning

This section shows the case of selecting optimal numbers and locations of PVRCs in CA to process EOL PV modules expected to retire during 2031 ~ 2035 (i.e. modules installed in Prospective period). Based on the waste prognosis, recycling facilities capable of processing total 1,300 MW per year PV EOL waste is suggested. Since, eight PVRCs are already constructed from Phase I and Phase II for processing total 700 MW capacity of PV wastes, new PVRCs for processing additional 600 MW (i.e 45,000 tonne) of EOL PV waste per year are required. Table 4.4 shows that the optimal numbers and locations of

new additional PVRC (different sizes) can be selected based on the size of PV waste generated in the prospective period, TTD, capacity limit of PVRC, and recycling costs.

Table 0.4: Total costs and emission generated from the Phase III planning.

# of new PVRC	Capacity (mT/year/PVRC)	TTD (10 ⁶ km)	Capital (\$M)	O&M (\$M)	Transport (\$M)	Total Cost (\$M)	GWP (10 ³ ton-CO ₂ eq)
3	16,000	20.8	3.8	24.3	13.6	41.7	3,062
4	12,000	18.8	4.3	25.6	12.3	42.2	2,759
6	8,000	17.9	5.1	27.2	11.2	43.5	2,491
8	6,000	16.9	5.7	28.2	10.4	44.3	2,296

Figure 4.7 shows the further breakdown of the total system costs in Phase III. Horizontal axis shows the number of additional PVRC constructed in Phase III and the breakdown of costs for capital (C), O&M (O), and transportation (T). Vertical axis in the left is the total system costs and each bar indicates the amount of cost components. Significant PV recycling processing capacity is already built in the Phase I and II. Therefore, additional capital costs for building, land, and equipment are only required for the new construction of PVRC in Phase III. Whereas, all PVRCs constructed in Phases I, II, and III still needs to operate fully. Therefore, unlike phase I and II, processing costs contribute significantly higher relative to the capital costs for the Phase III's total system costs. Vertical axis on the right shows the variation of percentile contribution of capital, transportation, and O&M costs to the total system cost in Phase III planning.

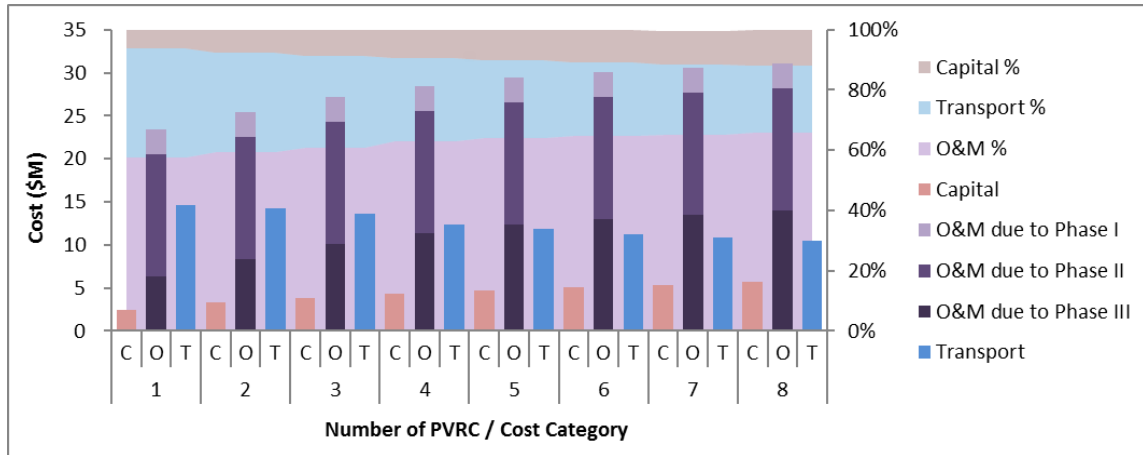


Figure 0.7: Total system cost vs. number of additional PVRCs in Phase III.

To show the effectiveness of the model, we took a conservative approach and picked allocating six additional PVRCs in the optimal decentralized locations (i.e. processing capacity of 8,000 tonne per year) in this phase. Figure 4.8 shows the geographical location of different size of PVIS installed in Saturation periods. It also shows the latitude and longitude of existing eight PVRCs constructed in Phase I and II along with additional 6 PVRCs constructed in Phase III. Other numbers of PVRC map can be found in appendix A-3.

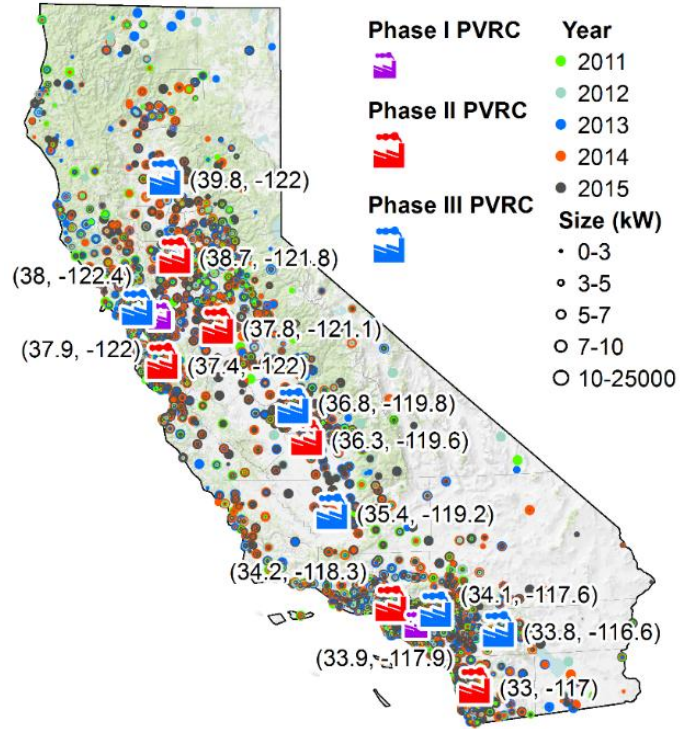


Figure 0.8: Six PVRCs selected for Phase III (2031 - 2035).

4.5 GIS Optimization

The method described in section 2.1.5 was used to locate PVRCs in the state of California for Phase I planning. In this research, the state of California was evenly divided to several individual areas based on the amount of PVIS. The median center of each area was computed separated. As a result, the geographical location of PVRC and the total transportation distance of each scenario were concluded.

Table 4.5 shows the transportation distance calculated by Matlab and GIS for Phase I planning. It was concluded that the distance results concluded by two methods are similar when the number of PVRC are less. The difference was larger when the number of PVRC

are getting more. The reason of that caused by the area dividing by human. Human area dividing is in an acceptable range when the number of area are less.

In addition, no area dividing is needed when locating one PVRC. So the results by two methods are supposed to be identical. The -2% difference is because the number of trip n_i was not able to be included in the GIS method. So a 2% was added in each scenario to revise the difference due to the number of trip.

In conclusion, GIS is a good way to approximate the locations and the total transportation distance when the target number of PVRC is less. The method is accurate enough with the error less than 5%. The method is also relatively easy to implement because no computer programming is required. As the number of PVRC increases, GIS is not recommended to use for approximation.

Table 0.5: Transportation distance by Matlab and GIS

Number of PVRC	Matlab Distance (10^6 km)	GIS Distance (10^6 km)	% Difference	Revised % Difference
1	9.45	9.23	-2%	0%
2	3.49	3.55	2%	4%
3	3.02	3.03	0%	3%
4	2.56	2.53	-1%	1%
5	2.13	2.22	4%	6%
6	1.87	1.95	4%	7%
7	1.69	1.97	16%	19%
8	1.55	1.75	13%	16%
9	1.46	1.80	23%	25%
10	1.36	1.58	16%	18%

CHAPTER V

OPTIMAL DISTRIBUTION MODEL

5.1 Model Description

A mathematical modeling framework was developed to generate the optimal distribution scheme by minimizing the transportation cost. In the framework, three parameters are included: 1) PVIS; 2) PVRC; and 3) TC. The mechanism of the recycling network is shown in Figure 5.1. The optimization is on a combinatorial problem. As a result, the optimal distribution scheme is presented by showing each PVIS is transported by which TC, and goes to which PVRC. The maximum annual capacity of each PVRC and TC are constraints to affect the distribution decision. Besides, the total transportation cost of the optimal distribution scheme can be conducted. Furthermore, the framework can show the amount of EoL PV that each PVRC received in each year to facilitate operational shift scheduling.

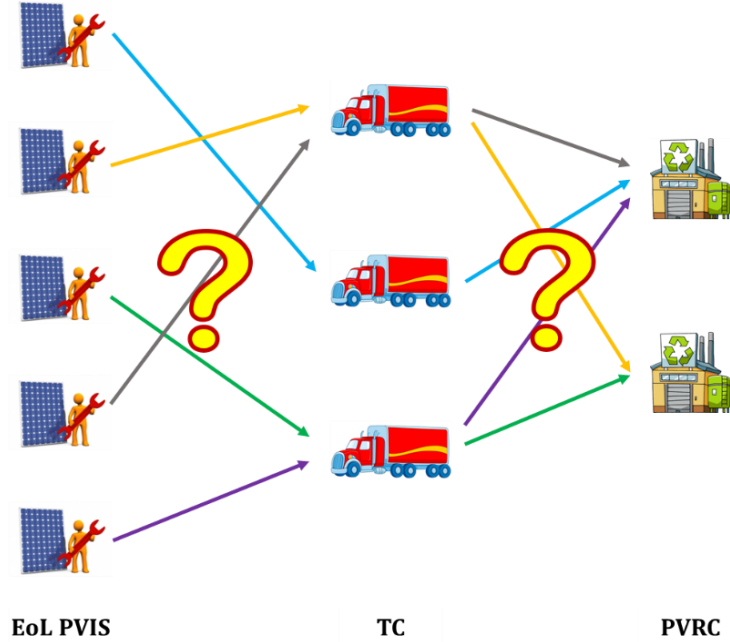


Figure 0.1: Mechanism of recycling network

Three types of data are required as input of the framework. The first input is the cost structure of TC, including the overhead cost, the unit mileage cost, and the unit weight cost. The overhead cost (\$/trip) is a fixed expense to start the transportation service. The mileage cost is obtained as the product of the unit mileage cost (\$/km) and the mileage (km) traveled. The weight cost is obtained as the product of the unit weight cost (\$/kg) and the weight of the material (kg) transported. The total cost of each transportation service is the summation of the overhead cost, the mileage cost, and the weight cost. The second input is the distance matrices consisting of a set of distance combination among PVIS, TC, and PVRC. With the latitude and the longitude of each PVIS, TC, and PVRC, the distance combination between two of three locations can be calculated and expressed in matrix forms. The third input is the size of each PVIS, TC, and PVRC. The weight of material of

each PVIS affects the weight cost. The annual capacity of each TC and PVRC is physical constraints affect the distribution result.

Two types of optimization algorithms were used in the modeling framework: a static optimization algorithm, and a dynamic optimization algorithm.

5.2 Static Optimization Algorithm

The static optimization algorithm is a type of the greedy algorithm (GA). GA is an algorithm of finding the optimal solution by using heuristic, which orders inputs by a seemingly logical way. In theory, as long as all inputs are ordered in the special way, the GA makes the same decisions that the optimal solution does. In practice, the optimal solution obtained by GA is most likely a local optimum. However, the local optimum solution is sometimes very close to the global optimum with significant amount of running time reduction.

The mechanism of GA in this model is shown in Figure 5.2. In the module, all PVIS can be sorted by their sizes from the largest to the smallest. The explanation is that the larger PVIS are the ones that would save the most money by choosing the cheapest transportation option. After sorting the size of PVIS, the largest PVIS has the first priority to be recycled by the first TC that offers the cheapest price. The less size PVIS has, the later that PVIS will be considered by the GA. As a result, for PVIS with larger size, the cost on transportation of that is the minimal. Though the saving of each is less, the total saving can add up by considering some thousands of PVIS. The annual capacity of PVRC and TC were included in the model as constraints.

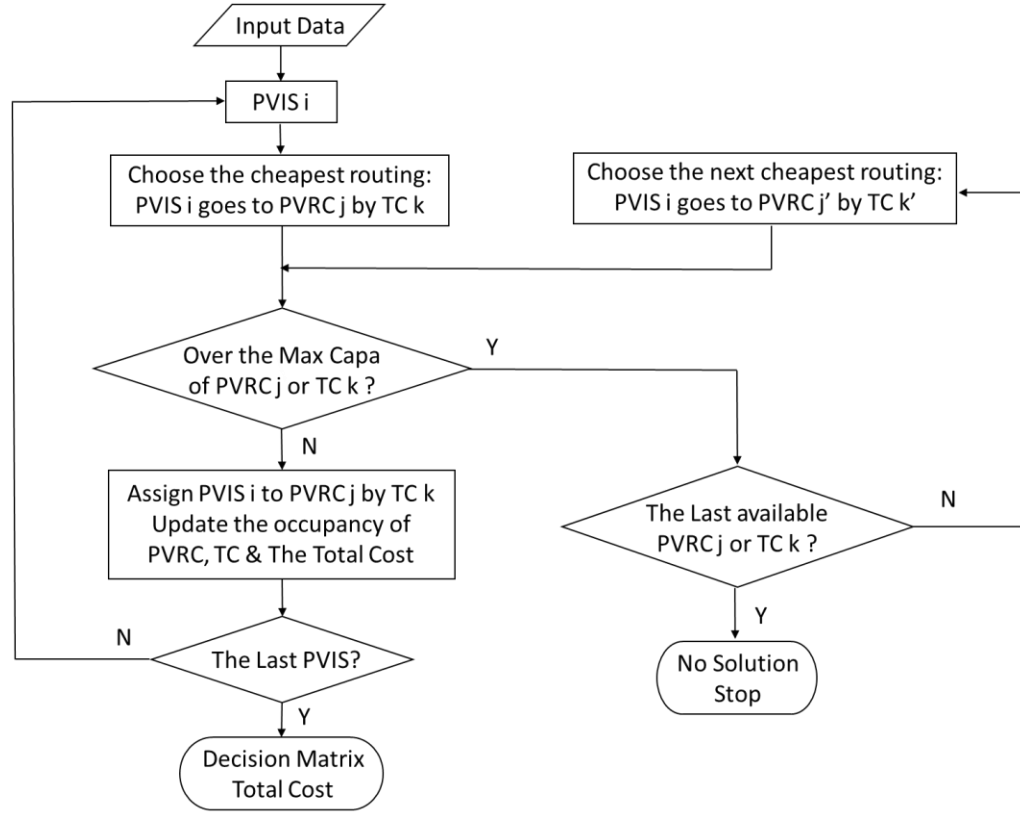


Figure 0.2: Mechanism of GA

5.3 Dynamic Optimization Algorithm

The dynamic optimization algorithm solves the problem by using the mixed integer linear programming. The objective function is equation 5.1, which minimizes the total transportation cost. Equation 5.2 is the summation of the transportation costs (overhead cost, mileage cost, and weight cost) from TC to PVIS, then to PVRC. Constraint 5.3 is to ensure all installed PVIS are sent as a whole to one of a PVRC. The linear inequalities in constraint 5.4 restrict that the total weight that each PVRC received is less than its maximum capacity. The linear inequalities in constraint 5.5 ensure that the total weight of

each TC transports is less than its maximum transportation capacity. The model iterates until it identifies the minimum total transportation cost.

Minimize

$$\sum_{i \in I} \sum_{j \in J} \sum_{k \in K} \{ [o_k \times n_i + m_k \times (D_{ki} + D_{ij} + D_{jk}) \times n_i + w_k \times W_i] \times Y_{ijk} \} \quad (5.1)$$

Subject to

$$\sum_{j \in J} \sum_{k \in K} Y_{ijk} = 1 \quad (5.2)$$

$$\sum_{i \in I} \sum_{k \in K} W_i Y_{ijk} \leq C_j \quad (5.3)$$

$$\sum_{i \in I} \sum_{j \in J} W_i Y_{ijk} \leq C_k \quad (5.4)$$

CHAPTER VI

CASE STUDY OF OPTIMAL DISTRIBUTION MODEL

6.1 Data Description

A case of California is considered to show the efficacy of the proposed framework in chapter VI. The State of California was selected because of its relatively long history and the significant amount of PV installations compared to other states. In addition, the preliminary recycling plan and the optimal locations of PVRC has been recommended by a previous study (cite our 1st paper). In the study, three recycling periods were recommended for recycling the EoL PV between the year 1984 – 2015 based on the amount of EoL PV as well as the increasing trend in each year. The location as well as the annual capacity of PVRC in each period was recommended as well: two 2,600 tonne annual capacity PVRC in Period I, addition six 8,000 tonne in Period II and addition six 40,000 tonne in Period III, respectively. The dispersion and the geographical locations of PVIS and PVRC in each recycling period are show is Figure 6.1.

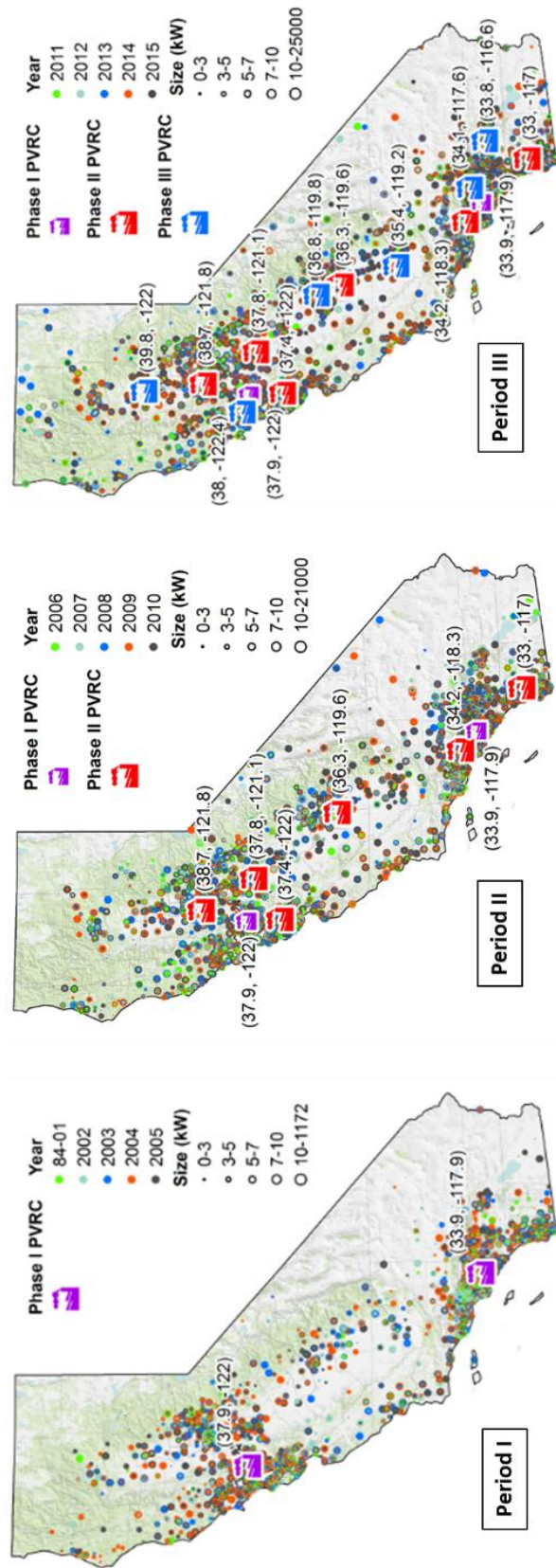


Figure 0.1: Locations of PVIS and PVRC in each recycling period

The annual PV Installations of California was shown in Figure 6.2. The figure shows the number of PVIS of each size range, as well as their size percentage among the total size of in each year. Three recycling periods were divided based on the number of PVIS as well as their total amount (kW) of each year. The first period has less quantity, as well as small amount of PVIS. The second period is the next. And the third period has the most quantity, as well as the most amount. Another insight of figure 6.2 is the number of PVIS in each kW range is not proportional with its total kW percentage. For instance, the size range of 3-10 kW contains the most number of PVIS (>70%) from the year of 2009 to the year of 2012. However, the total kW of that size range of PVIS are less than 30%. In the opposite, the number of PVIS in size range of 100-1,200 kW can be barely counted. However, they account for about 50% of the total kW amount. In conclusion, the small size (3-10 kW) PVIS are dominated in the quantity perspective, but in the overall amount of kW perspective, the proportion of larger size (100-2500 kW) PVIS is not negligible.

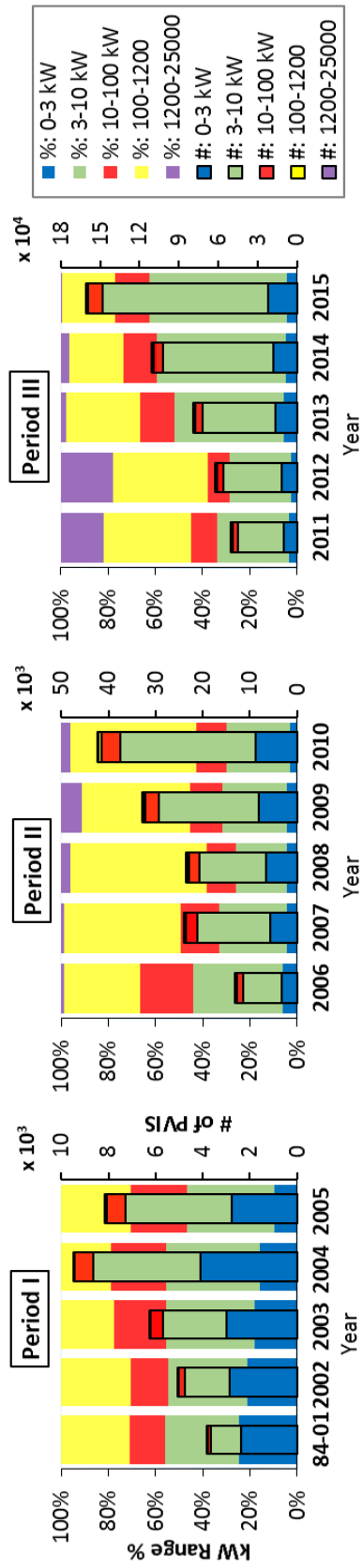


Figure 0.2: Annual PV installations in California (1984 – 2015)

6.2 Optimization Algorithm Application

The following assumptions are made for the modeling: the maximum load of a truck is 7.5 metric tons; approximate weight of material of every 1 MW capacity PV modules are equivalent to 75 metric tons [32]; With the above assumptions, each truck can take at most 100 kW PV modules. Considering the significant percentage (about 40%, in figure 6.2) of PV modules that are over 100 kW, the number trips of transporting them is non-neglectable.

In reality, due to the competitive market, the price of each TC offers tends to be similar. In addition, the mileage of the truck driving from a TC to a PVIS, and the mileage of the truck driving away from a TC to a PVIS are dead mileage. Dead mileage is usually not to be charged in reality. Thus, the optimization process is no longer related to TC. Consequently, the transportation cost function of recycling each individual PVIS in both the static and the dynamic algorithms can be simplified in terms of the overhead cost, o , the unit mileage cost m , the unit weight cost, w , the travel distance between the PVIS and the PVRC, D , the weight of material of the PVIS, W , and the number of trips, n , and is shown in equation 6.1. By using the simplified cost function, variables in optimization processes can be reduced by at least 50%.

$$\text{Transportation cost} = o \times n + m \times D \times n + w \times W \quad (6.1)$$

With the simplification, the dynamic optimization algorithm was simplified as:

Minimize

$$\sum_{i \in I} \sum_{j \in J} \{[o \times n_i + m \times D_{ij} \times n_i + w \times W_i] \times Y_{ij}\} \quad (6.2)$$

Subject to

$$\sum_{j \in J} Y_{ij} = 1 \quad (6.3)$$

$$\sum_{i \in I} W_i Y_{ij} \leq C_j \quad (6.4)$$

The simplified form can improve the feasibility for handling larger number of PVIS and fasten the computational speed of MILP. In addition, rather than MILP, Linear Program (LP) is recommended and utilized for solving the particular California case. It is concluded that LP is able to handle more variables, compute and converge way faster, and conduct the total transportation cost with the error of less than 1% of the total transportation cost conducted by the MILP.

While performing the optimization with both algorithms, the following unit costs were utilized: the overhead cost is \$10/trip, the unit mileage cost is \$0.06/km, and the unit weight cost is \$0.008/kg. The accuracy of each type of unit cost is not critical as the research is dedicating to construct a generic framework that providing the optimal distribution scheme with the objective of minimizing the total transportation cost. The framework can be employed in any multi-facility recycling problem in anywhere as long as the unit cost rates are available.

6.3 Results

Matlab was utilized as the tool to perform the optimization for both algorithms. The baseline total transportation cost, and the optimal total transportation cost conducted by the GA and the LP is shown in figure 6.3. The baseline cost indicates the total transportation cost of recycling PVIS by their installed date without doing any optimization. In that way, each PVIS is going to the closest PVRC whose maximum annual capacity has not been reached. The transportation cost conducted by GA and LP is the optimal cost as they are generated by optimization processes. The mechanism of the GA is recycling PVIS from the largest size to the smallest while, LP processes the optimization with the objective of minimizing the overall transportation cost.

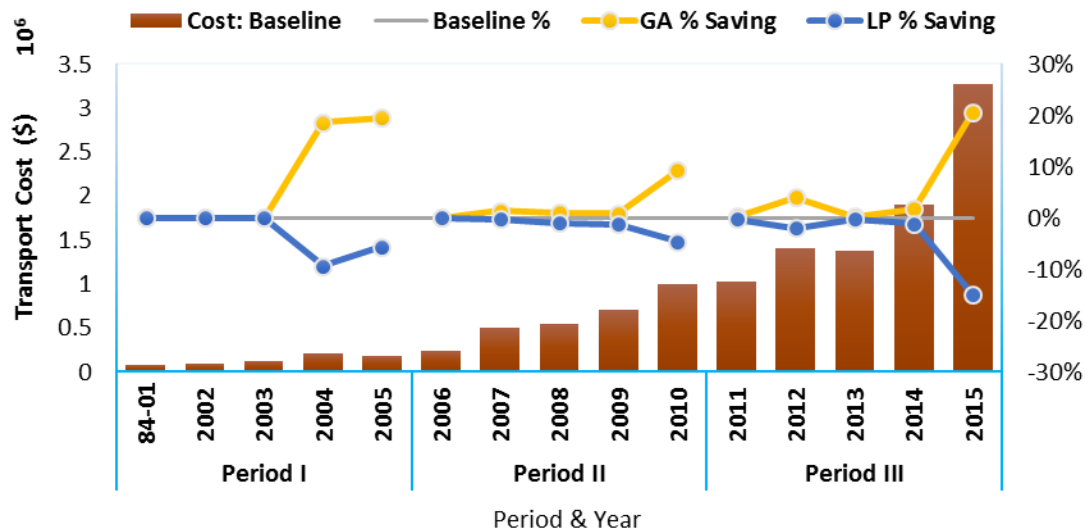


Figure 0.3: Transportation cost and saving by each method and year

Ideally, LP provides the lowest optimal cost, but also with the most computational expense. The optimal cost that GA provided is higher than LP, but lower than the baseline cost. However, in figure 6.3, GA even costs more than baseline. The reason of that is

because of the specialty of the size distribution of CA PVIS as well as the effect of the hypothesis cost structure. Table 6.1 shows the combination of transporting the total 100 kW, 300 kW, and 500 kW PVIS for 100 km. In that, 100 of 1kW, 10 of 10 kW, and 1 of 100 kW of PVIS was for the total 100 kW and the same logic for the total 300 kW, and 500 kW of PVIS. It shows that due to the large percentage of the overhead cost among the grand total, the cost of transporting 100 of 1 kW is 21.8 times expensive than transporting 1 of 100 kW, and 7.8 and 5.0 times expensive for the 300 kW and 500 kW case. Thus, small size PVIS should be considered first for saving the most money. In addition, from figure 6.2, the number of PVIS with the size in between 0-10 kW accounts for about 90% of the total. In conclusion, for recycling PVIS in CA with the current hypothesis cost structure, having small size PVIS get recycled by the cheapest way is the way to maximize the total transportation cost saving. Therefore, GA should be modified as sorting the size of PVIS from the smallest to the largest and assign the cheapest transport option to smaller PVIS first and was denoted as GA'.

Table 0.1: Total cost and multiple PVIS Size and quantity combination

PVIS Size (kW)	# of Trips	Overhead Cost (\$)	Mileage Cost (\$)	Weight Cost (\$)	Grand Total (\$)	# of PVIS	Total Cost (\$)	Multiple
1	1	10	6	0.6	17	100	1660	21.8
10	1	10	6	6	22	10	220	2.9
100	1	10	6	60	76	1	76	1.0
3	1	10	6	1.8	18	100	1780	7.8
30	1	10	6	18	34	10	340	1.5
300	3	30	18	180	228	1	228	1.0
5	1	10	6	3	19	100	1900	5.0
50	1	10	6	30	46	10	460	1.2
500	5	50	30	300	380	1	380	1.0

Table 6.2 shows the transportation cost savings by the modified GA (GA') and LP of each year. There are two conclusions. First, saving only appears in those years where the annual capacity of PVRC is relative tight compare with the amount of PV needs to be recycled (amount of installed PV). The tighter annual capacity of PVRC, the more saving is expected by doing optimization. No savings when the annual capacity of PVRC is about two or more times than the amount of PV needs to be recycled. Second, the saving difference between GA' and LP in each scenario are trivial. However, the computational of LP could be way longer than GA', especially when the number of PVIS and PVRC both increases significantly. The computation time of LP for the year 2015 is as high as 3.5 hours. Third, the number of PVIS is another factor affects the saving. The amount of installed PV in the year of 2004 is less than the year of 2005. However, the saving of the year 2004 is twice of the year 2005. The reason of that is the number of PVIS in the year of 2004 is about one third more than 2005 as shown in figure 6.2. Based on above

conclusion, in the CA case, it is reasonable to rely on the solution generated by GA' with a relative accurate solution, a short running time than LP, without purchasing an optimization solver.

Table 0.2: Saving of GA' and LP of each year

Period	PVRC Recycling Capacity (MW/yr)	Installed Year	Amount of Installed PV (MW)	GA' Saving (\$K)	LP Saving (\$K)	Computation Time Ratio (LP/GA')
I	70	84-01	19	0	0	11
		2002	29	0	0	15
		2003	40	0	0	14
		2004	63	20	20	15
		2005	65	10	10	15
II	700	2006	113	0	0	70
		2007	287	2	2	152
		2008	346	5	5	148
		2009	418	8	9	235
		2010	603	44	45	311
III	1,300	2011	643	2	2	869
		2012	953	26	27	1,187
		2013	671	3	3	1,506
		2014	866	20	22	2,544
		2015	1216	473	491	3,731

From table 6.2, though the saving can be as high as \$491,000 for transporting EoL PV installed in the year 2015, the saving is not significant in percentage perspective (15%). The applied cost structure is a factor affects the saving percentage. Equation 6.1 (Cost Structure 1) was used in the simulation. In that cost structure, only the mileage cost can be reduced by optimization and neither the overhead cost nor the weight cost. In order to show the importance of the planning, Cost Structure 2 in equation 5.5 was hypothesized so that

the transportation cost is only related to the unit mileage cost, m , the travel distance, D , and the number of trip, n . Assume the unit mileage cost is \$0.2/km.

$$\text{Transportation cost} = m \times D \times n \quad (6.5)$$

Table 6.3 shows the saving comparison that generated by different cost structure of each year. From the table, savings turns to be significant, at most 50%, especially when the annual capacity of PVRC is tight. Therefore, well planning is beneficial.

Table 0.3: Percentage saving of in each cost structure of each year

Period	Installed Year	Cost Structure 1		Cost Structure 2	
		GA' % Saving	LP % Saving	GA' % Saving	LP % Saving
I	84-01	0%	0%	0%	0%
	2002	0%	0%	0%	0%
	2003	0%	0%	0%	0%
	2004	9%	9%	24%	25%
	2005	5%	6%	16%	16%
II	2006	0%	0%	0%	0%
	2007	0%	0%	2%	3%
	2008	1%	1%	6%	6%
	2009	1%	1%	7%	8%
	2010	4%	5%	25%	26%
III	2011	0%	0%	1%	1%
	2012	2%	2%	15%	16%
	2013	0%	0%	2%	2%
	2014	1%	1%	8%	8%
	2015	14%	15%	51%	53%

The distribution decision by GA' was displayed on maps by GIS and shown in figure 6.4. The installed year 2003, 2008, and 2013 were selected to represent the installed period I, II, and III. PVIS were assigned to the closest, none-full PVRC.

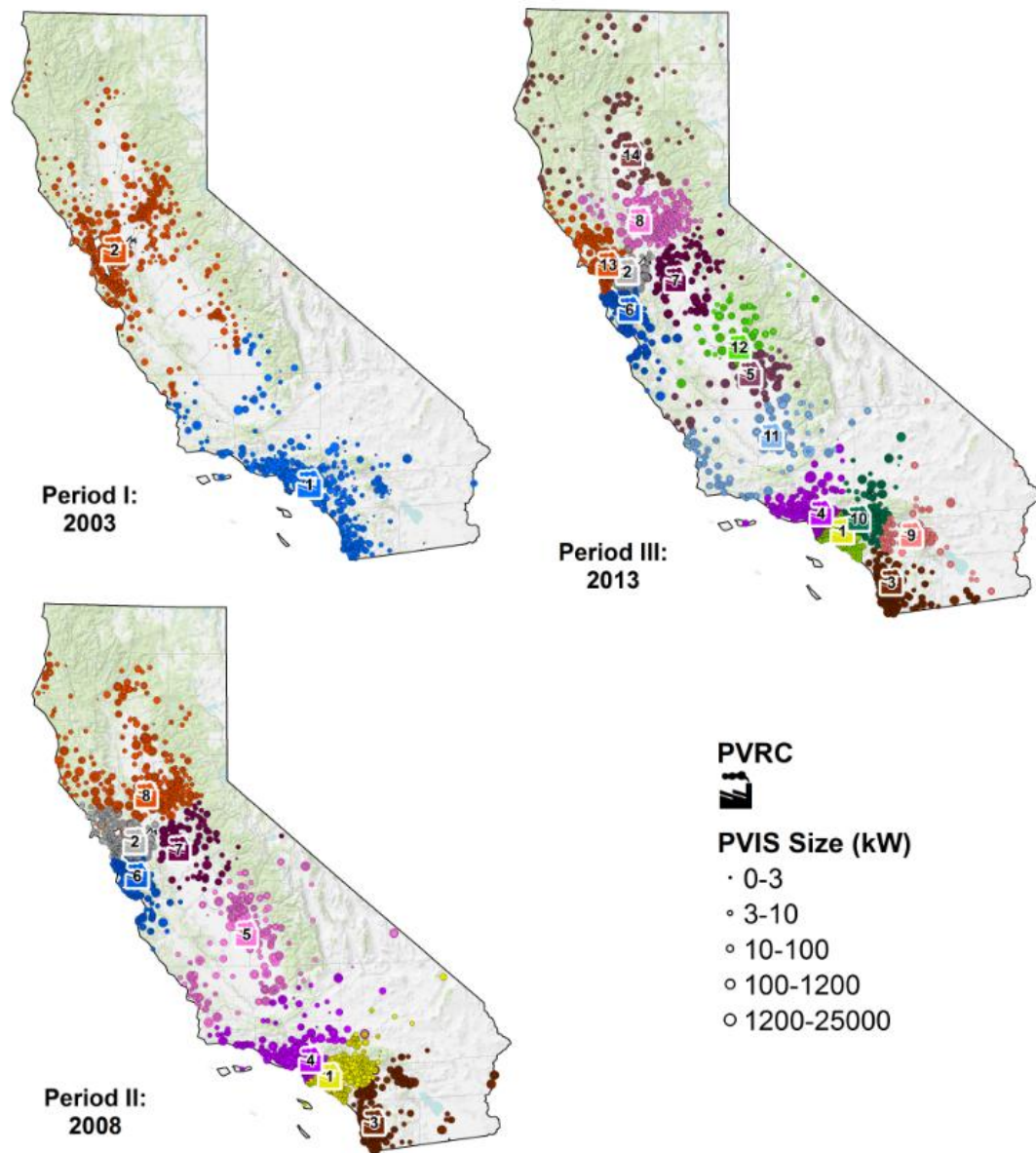


Figure 0.4: Distribution decision of year 2003, 2008, and 2013

Table 6.4 shows the amount of EoL PV module each PVRC received for installed year 2003, 2008, and 2013. The serial number of each PVRC was shown in figure 6.4. The occupancy percentage of each PVRC can help on employee shift scheduling.

Table 0.4: Amount of EoL PV each PVRC receives each year

PVRC Serial #	2003		2008		2013		Max Annual Capacity (MW)
	Amount (MW)	%	Amount (MW)	%	Amount (MW)	%	
1	19	54%	35	100%	35	100%	35
2	21	60%	35	99%	35	99%	35
3	-	-	47	45%	79	76%	105
4	-	-	56	54%	96	92%	105
5	-	-	47	45%	32	30%	105
6	-	-	59	56%	68	65%	105
7	-	-	12	11%	28	27%	105
8	-	-	56	53%	53	50%	105
9	-	-	-	-	43	43%	100
10	-	-	-	-	61	61%	100
11	-	-	-	-	45	45%	100
12	-	-	-	-	36	36%	100
13	-	-	-	-	44	44%	100
14	-	-	-	-	17	17%	100

CHAPTER VII

CONCLUSION AND FUTURE WORK

The multi-facility optimization model was developed to solve a location allocation problem of minimizing the system cost for recycling PV in the state of California. The geographical locations of potential PVRCs were found for three different phases (short, mid, and long terms). Total transportation distance, the total cost, and the environmental impact of each phase of recycle planning were concluded. The analysis indicated that two PVRCs scenario has the highest cost-effectiveness in phase I. Additional six PVRCs are recommended in both phases II and III. Although the analysis was performed based on the PV installation data in the state of California, the proposed model can be applied to any geographical area. The optimal solutions generated by the model can provide valuable insights for policymakers and stakeholders to initiate the PV recycling in the United States.

Rather than the mathematical way, GIS can be used to approximate the locations and the total transportation distance with a decent accurate when the target number of PVRC is less. The method is also relatively easy to implement because no computer programming is required. As the number of PVRC increases, GIS is not recommended to use for approximation.

In addition, optimal distribution model was constructed to generate the optimal distribution scheme for transporting EoL PVIS. A static and a dynamic optimization algorithm, GA and LP, respectively was employed in the framework. The following conclusions were concluded from the simulation result based on the PV installed case in CA. First, based on the size distribution of PV installed in CA, the focus of the optimization should be on small size PVIS than large sizes. The most saving is obtained by optimizing transport distribution on small size PVIS. Second, GA is a reliable algorithm to perform the transporting distribution optimization with a decent accuracy, low computational cost, no optimization solver required for the CA case. Third, no saving achieved, thus no optimization needed when the annual recycling capacity of PVRC is twice or larger than the amount of the recycled PV demand. Saving increases with the annual capacity of PVRC getting tighter. With the appropriate optimization process and the specific cost structure applied, savings can be expected at most 53% compare with not doing optimization. The developed framework has a wide applicability and can be applied on any PV recycling case for reducing the transportation cost.

Future work can focus on further reducing the transportation cost by maximizing the truck occupancy of each trip. From figure 6.2, 90% of PVIS has the size less than 10 kW, equals to 0.75 metric tons. The hypothesized truck load is 7.5 metric tons. So each truck can take at least 10 PVIS with the size 0-10 kW. With this estimation, about another 90% saving can be expected on top of the current saving. In order to achieve that, rather than the installed location, the installed date of each PVIS should be considered to evaluate the possibility of transport several EoL PV module in one trip. Also, a multi-objective

optimization model needs to be developed by minimizing the transportation cost and minimizing the environmental impact (maximizing the truck load).

BIBLIOGRAPHY

1. Fthenakis, V., *Sustainability of photovoltaics: The case for thin-film solar cells*. Renewable and Sustainable Energy Reviews, 2009. **13**(9): p. 2746-2750.
2. Choi, J.-K. and Fthenakis, V., *Crystalline silicon photovoltaic recycling planning: macro and micro perspectives*. Journal of Cleaner Production, 2014. **66**: p. 443-449.
3. EPIA, *Global Market Outlook for Solar Power 2016-2020*. 2016.
4. SEIA, *Solar Market Insight Report 2016 Year In Review*. 2017.
5. Fthenakis, V. and Kim, H.C., *Land use and electricity generation: A life-cycle analysis*. Renewable and Sustainable Energy Reviews, 2009. **13**(6–7): p. 1465-1474.
6. Sims, R.E.H., Rogner, H.-H., and Gregory, K., *Carbon emission and mitigation cost comparisons between fossil fuel, nuclear and renewable energy resources for electricity generation*. Energy Policy, 2003. **31**(13): p. 1315-1326.
7. Choi, J.-K., *Waste Prognosis of the Photovoltaic Waste in the United States*, in *Technical Report* 2015, University of Dayton.
8. Goe, M. and Gaustad, G., *Identifying critical materials for photovoltaics in the US: A multi-metric approach*. Applied Energy, 2014. **123**: p. 387-396.
9. Bustamante, M.L. and Gaustad, G., *Challenges in assessment of clean energy supply-chains based on byproduct minerals: A case study of tellurium use in thin film photovoltaics*. Applied Energy, 2014. **123**: p. 397-414.
10. Cucchiella, F., D'Adamo, I., and Rosa, P., *End-of-Life of used photovoltaic modules: A financial analysis*. Renewable and Sustainable Energy Reviews, 2015. **47**: p. 552-561.

11. Sener, C. and Fthenakis, V., *Energy policy and financing options to achieve solar energy grid penetration targets: Accounting for external costs*. Renewable and Sustainable Energy Reviews, 2014. **32**: p. 854-868.
12. EPIA. *Global Market outlook for photovoltaics 2014~2018*. 2013; Available from: http://ec.europa.eu/economy_finance/events/2009/20091120/epia_en.pdf.
13. Du, X. and Graedel, T.E., *Global In-Use Stocks of the Rare Earth Elements: A First Estimate*. Environmental Science & Technology, 2011. **45**(9): p. 4096-4101.
14. McDonald, N.C. and Pearce, J.M., *Producer responsibility and recycling solar photovoltaic modules*. Energy Policy, 2010. **38**(11): p. 7041-7047.
15. Goe, M. and Gaustad, G., *Strengthening the case for recycling photovoltaics: An energy payback analysis*. Applied Energy, 2014. **120**: p. 41-48.
16. AgencyforToxicSubstancesandDiseaseRegistry, *CERCLA Priority List of Hazardous Substances*, Registry, U.D.o.H.a.H.S.A.f.T.S.a.D., Editor 2007.
17. Fthenakis, V.M., *End-of-life management and recycling of PV modules*. Energy Policy, 2000. **28**: p. 1051-1058.
18. Williams, E.D., Ayres, R.U., and Heller, M., *The 1.7 Kilogram Microchip: Energy and Material Use in the Production of Semiconductor Devices*. Environmental Science & Technology, 2002. **36**(24): p. 5504-5510.
19. Fthenakis, V., *Sustainability metrics for extending thin-film photovoltaics to terawatt levels*. MRS Bulletin, 2012. **37**(04): p. 425-430.
20. Larsen, K., *End-of-life PV: then what?* Renewable Energy Focus, 2009. **10**(4): p. 48-53.
21. Berger, W., Simon, F.-G., Weimann, K., and Alsema, E.A., *A novel approach for the recycling of thin film photovoltaic modules*. Resources, Conservation and Recycling, 2010. **54**(10): p. 711-718.
22. Hosenuzzaman, M., Rahim, N.A., Selvaraj, J., Hasanuzzaman, M., Malek, A.B.M.A., and Nahar, A., *Global prospects, progress, policies, and environmental impact of solar photovoltaic power generation*. Renewable and Sustainable Energy Reviews, 2015. **41**: p. 284-297.
23. Zhong, Z.W., Song, B., and Loh, P.E., *LCAs of a polycrystalline photovoltaic module and a wind turbine*. Renewable Energy, 2011. **36**(8): p. 2227-2237.

24. Choi, J.-K., Stuart, J.A., Ramani, K., *Modeling of automotive recycling planning in the United States*. International Journal of Automotive Technology, 2005. **6**(4): p. 413-419.
25. Choi, J.-K., Kelley, D., Murphy, S., and Thangamani, D., *Economic and environmental perspectives of end-of-life ship management*. Resources, Conservation and Recycling, 2016. **107**: p. 82-91.
26. Choi, J.-K. and Fthenakis, V., *Design and Optimization of Photovoltaics Recycling Infrastructure*. Environmental Science & Technology, 2010. **44**(22): p. 8678-8683.
27. Goe, M., Gaustad, G., and Tomaszewski, B., *System tradeoffs in siting a solar photovoltaic material recovery infrastructure*. Journal of Environmental Management, 2015. **160**: p. 154-166.
28. Fthenakis, V.M. and Kim, H.C., *Photovoltaics: Life-cycle analyses*. Solar Energy, 2011. **85**(8): p. 1609-1628.
29. Giachetta, G., Leporini, M., and Marchetti, B., *Evaluation of the environmental benefits of new high value process for the management of the end of life thin film photovoltaic modules*. Journal of Cleaner Production, 2013. **51**: p. 214-224.
30. Wambach, K., *PV module take back and recycling systems in Europe: new challenges under WEEE*, in *27th European Photovoltaics Solar Energy Conference and Exhibition 2012*: Frankfurt, Germany.
31. PVCYCLE, *European Association for the Recovery of Photovoltaic Modules Annual Report 11*, 2011.
32. Choi, J.-K. and Fthenakis, V., *Economic Feasibility of Recycling Photovoltaic Modules*. Journal of Industrial Ecology, 2010. **14**(6): p. 947-964.
33. Rubio, S., Chamorro, A., and Miranda, F.J., *Characteristics of the research on reverse logistics (1995–2005)*. International Journal of Production Research, 2007. **46**(4): p. 1099-1120.
34. Fleischmann, M., Krikke, H.R., Dekker, R., and Flapper, S.D.P., *A characterisation of logistics networks for product recovery*. Omega, 2000. **28**(6): p. 653-666.
35. Srivastava, S.K., *Network design for reverse logistics*. Omega, 2008. **36**(4): p. 535-548.

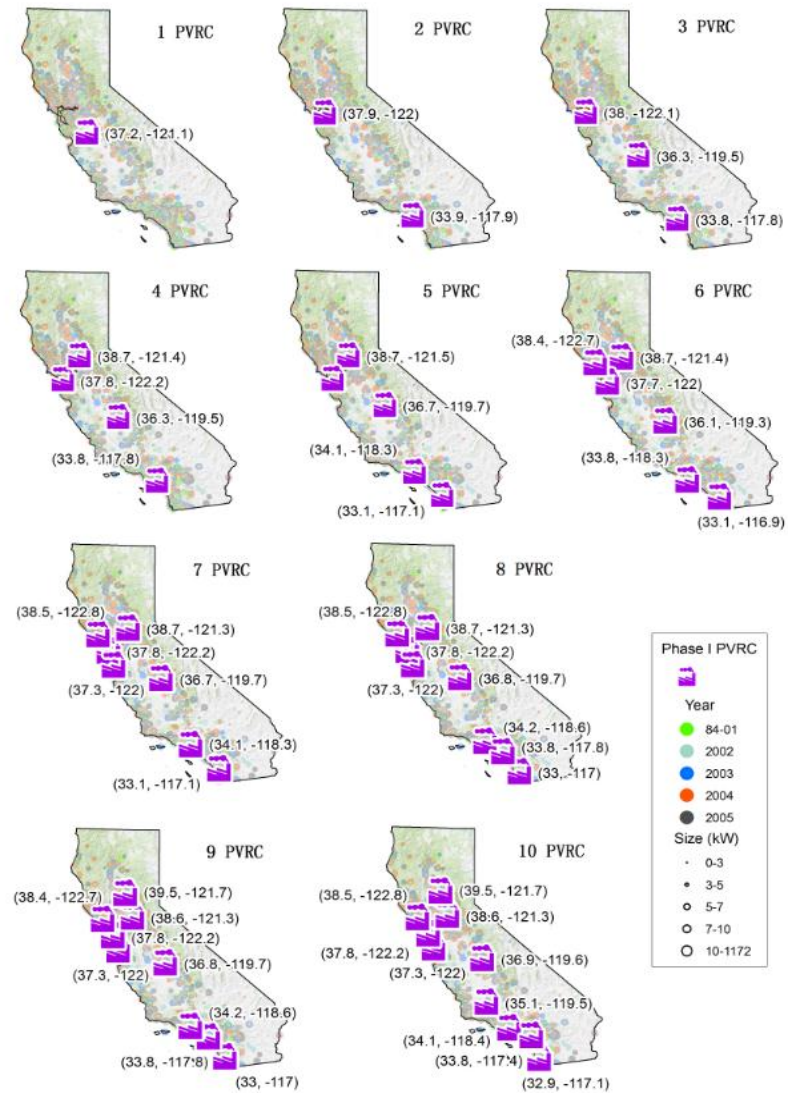
36. Min, H., Jeung Ko, H., and Seong Ko, C., *A genetic algorithm approach to developing the multi-echelon reverse logistics network for product returns*. Omega, 2006. **34**(1): p. 56-69.
37. Choi, J.-K., Sturat, J., and Ramani, K., *Modeling of automotive recycling planning in the United States*. International Journal of Automotive technology, 2005. **6**(4): p. 413-419.
38. Jena, S.D., Cordeau, J.-F., and Gendron, B., *Solving a Dynamic Facility Location Problem with an Application in Forestry*. 2014.
39. Louwers, D., Kip, B.J., Peters, E., Souren, F., and Flapper, S.D.P., *A facility location allocation model for reusing carpet materials*. Computers & Industrial Engineering, 1999. **36**(4): p. 855-869.
40. Iyigun, C. and Ben-Israel, A., *The multi-facility location problem: a probabilistic decomposition method*. Computational Optimization and Applications, 2013.
41. Rahmati, S.H.A., Hajipour, V., and Niaki, S.T.A., *A soft-computing Pareto-based meta-heuristic algorithm for a multi-objective multi-server facility location problem*. Applied Soft Computing, 2013. **13**(4): p. 1728-1740.
42. Tcha, D.-w. and Lee, B.-i., *A branch-and-bound algorithm for the multi-level uncapacitated facility location problem*. European Journal of Operational Research, 1984. **18**(1): p. 35-43.
43. Hu, T.-L., Sheu, J.-B., and Huang, K.-H., *A reverse logistics cost minimization model for the treatment of hazardous wastes*. Transportation Research Part E: Logistics and Transportation Review, 2002. **38**(6): p. 457-473.
44. Efendigil, T., Önüt, S., and Kongar, E., *A holistic approach for selecting a third-party reverse logistics provider in the presence of vagueness*. Computers & Industrial Engineering, 2008. **54**(2): p. 269-287.
45. Gölle, A., Görbe, P., and Magyar, A., *Modeling and optimization of electrical vehicle batteries in complex clean energy systems*. Journal of Cleaner Production, 2012. **34**: p. 138-145.
46. Daskin, M., Snyder, L., and Berger, R., *Facility Location in Supply Chain Design*, in *Logistics Systems: Design and Optimization*, Langevin, A. and Riopel, D., Editors. 2005, Springer US. p. 39-65.
47. Akhtar, M., Hannan, M.A., Begum, R.A., Basri, H., and Scavino, E., *Backtracking search algorithm in CVRP models for efficient solid waste collection and route optimization*. Waste Management, 2017. **61**: p. 117-128.

48. Kallel, A., Serbaji, M.M., and Zairi, M., *Using GIS-Based Tools for the Optimization of Solid Waste Collection and Transport: Case Study of Sfax City, Tunisia*. Journal of Engineering, 2016. **2016**: p. 7.
49. Zheng, Y.-J. and Ling, H.-F., *Emergency transportation planning in disaster relief supply chain management: a cooperative fuzzy optimization approach*. Soft Computing, 2013. **17**(7): p. 1301-1314.
50. Dotoli, M., Hammadi, S., Jeribi, K., Russo, C., and Zgaya, H. *A multi-agent Decision Support System for optimization of co-modal transportation route planning services*. in *52nd IEEE Conference on Decision and Control*. 2013.
51. Demirel, E., Demirel, N., and Gökçen, H., *A mixed integer linear programming model to optimize reverse logistics activities of end-of-life vehicles in Turkey*. Journal of Cleaner Production, 2016. **112**: p. 2101-2113.
52. Cao, Z., Guo, H., Zhang, J., Niyato, D., and Fastenrath, U., *Finding the Shortest Path in Stochastic Vehicle Routing: A Cardinality Minimization Approach*. IEEE Transactions on Intelligent Transportation Systems, 2016. **17**(6): p. 1688-1702.
53. Camino, J.T., Artigues, C., Houssin, L., and Mourgues, S. *Mixed-integer linear programming for multibeam satellite systems design: Application to the beam layout optimization*. in *2016 Annual IEEE Systems Conference (SysCon)*. 2016.
54. Dubois-Lacoste, J., Pagnozzi, F., and Stützle, T., *An iterated greedy algorithm with optimization of partial solutions for the makespan permutation flowshop problem*. Computers and Operations Research, 2017. **81**: p. 160-166.
55. Qin, J., Chow, Y., Yang, J., and Rajagopal, R., *Distributed Online Modified Greedy Algorithm for Networked Storage Operation Under Uncertainty*. IEEE Transactions on Smart Grid, 2016. **7**(2): p. 1106-1118.
56. Cerrone, C., Cerulli, R., and Golden, B., *Carousel greedy: A generalized greedy algorithm with applications in optimization*. Computers & Operations Research, 2017. **85**: p. 97-112.
57. Go Solar California. *California Solar Statistics, State of California*, <https://www.californiasolarstatistics.ca.gov/>. 2017.
58. SEIA. *State Solar Policy, California Solar*, <http://www.seia.org/state-solar-policy/california>. 2017.

59. UniversityofColoradoBoulder. *Calculation of Distance Represented by Degrees of Latitude and Longitude*. [cited 2015; Available from: <http://www.colorado.edu/geography/gcraft/warmup/aquifer/html/distance.html>].
60. Shumaker, B. and Sinnott, R., *Astronomical computing: 1. Computing under the open sky. 2. Virtues of the haversine*. Sky and telescope, 1984. **68**: p. 158-159.
61. MathWorks. *fmincon*. 2015 [cited 2015; Available from: <http://www.mathworks.com/help/optim/ug/fmincon.html>].
62. Wikipedia. *Maxima and minima*. 2014 [cited 2014; Available from: http://en.wikipedia.org/wiki/Maxima_and_minima].
63. MathWorks. *How to get the global minimum by fmincon* 2011 [cited 2015; Available from: http://www.mathworks.com/matlabcentral/newsreader/view_thread/307142].
64. Tsilemou, K. and Panagiotakopoulos, D., *Approximate cost functions for solid waste treatment facilities*. Waste management & research, 2006. **24**(4): p. 310-322.
65. Ecoinvent Centre, *Overview and Methodology*., in *Final report ecoinvent data V2.12009*, Swiss Centre for Life Cycle Inventories: Dubendorf, CH.
66. IPCC, *IPCC Fourth Assessment Report (AR4)*, 1, W.G., Editor 2007, Intergovernmental Panel on Climate Change.
67. McCarthy, K., *RESIDENTIAL SOLAR ENERGY PROGRAMS*, 2006.
68. Borenstein, S., *The California Solar Initiative is ending. What has it left behind?*, 2013.
69. Guevara-Stone, L., *California Flattens Rate Blocks, Rolls Out Default Time-of-use Pricing*, 2015.

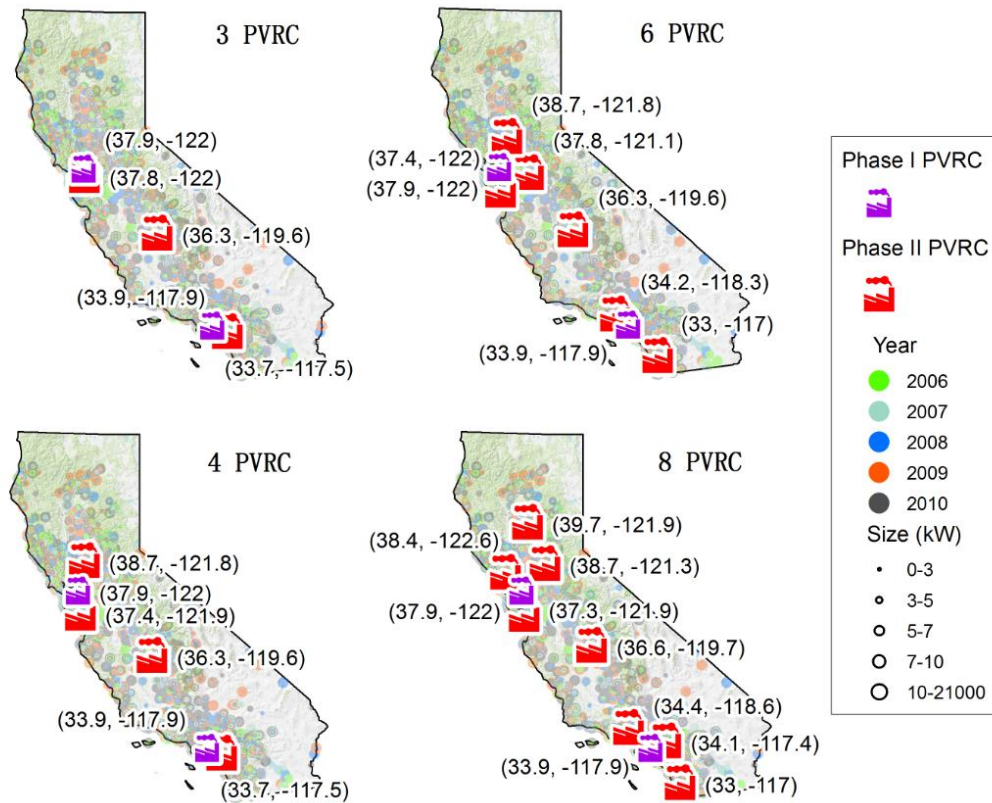
APPENDIX A-1

Location of PVRC in Phase I



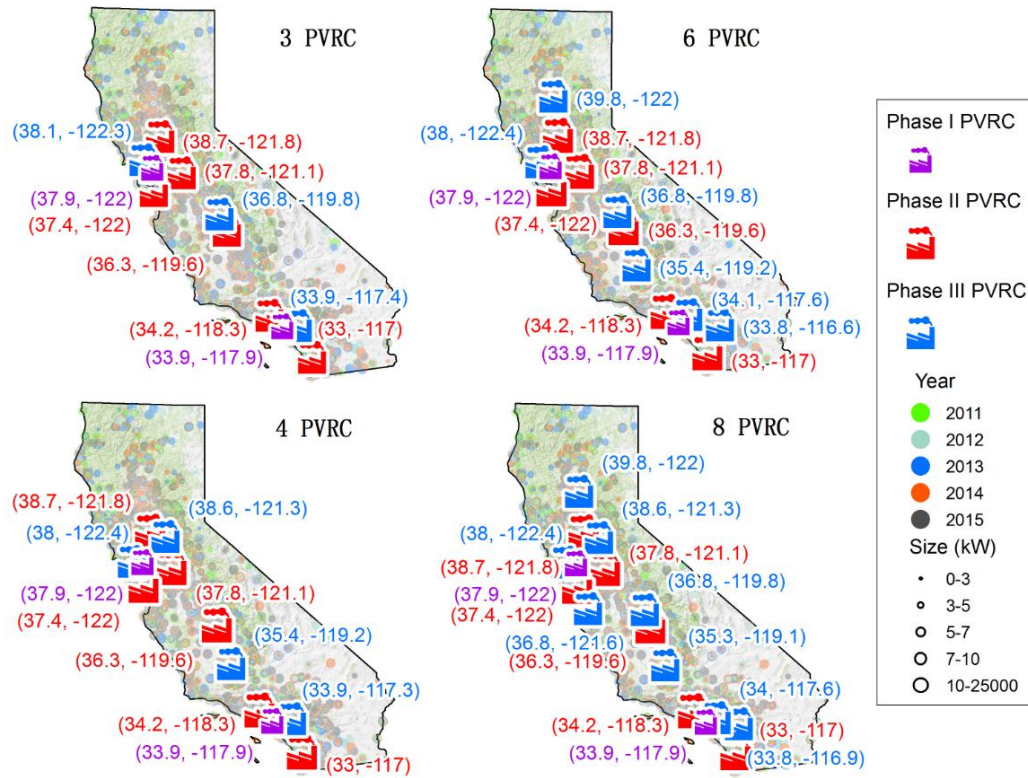
APPENDIX A-2

Location of PVRC in Phase II



APPENDIX A-3

Location of PVRC in Phase III



APPENDIX B

Large PVIS

Longitude	Latitude	Size(MW)	Year
-119.69	35.62	32	2013
-120.13	36.00	35	2013
-118.17	35.05	45	2013
-119.49	35.89	50	2013
-119.23	36.99	60	2013
-120.10	36.43	60	2013
-120.38	36.75	63	2013
-120.85	37.06	110	2013
-115.72	32.75	139	2013
-115.65	32.68	150	2013
-115.66	32.68	170	2013
-115.88	32.78	200	2013
-121.62	39.76	200	2013
-120.25	36.65	206	2013
-119.92	35.33	250	2013
-118.16	34.86	40	2014
-118.17	35.05	60	2014
-119.02	35.37	75	2014
-119.78	36.30	100	2014
-119.78	36.30	105	2014
-117.97	35.31	107	2014
-115.57	32.85	150	2014
-117.97	35.31	150	2014
-118.43	34.78	230	2014
-115.64	32.67	266	2014

-118.42	34.77	266	2014
-114.99	33.67	280	2014
-117.33	35.01	280	2014
-115.47	35.57	392	2014
-120.07	35.38	550	2014
-117.65	35.00	30	2015
-120.25	36.65	40	2015
-117.97	35.31	50	2015
-118.16	34.86	100	2015
-118.16	34.86	110	2015
-118.16	34.86	279	2015
-115.40	33.83	550	2015
-118.40	34.83	579	2015
-117.65	35.00	30	2016
-117.65	35.00	30	2016
-117.65	35.00	30	2016
-117.20	34.93	30	2016
-115.99	32.74	30	2016
-118.15	34.69	50	2016
-117.97	35.31	56	2016
-118.16	34.86	75	2016
-117.65	35.00	80	2016
-117.20	34.93	80	2016
-118.15	34.69	85	2016
-115.27	35.47	126	2016
-115.50	32.68	130	2016
-115.27	35.47	133	2016
-115.27	35.47	133	2016
-115.78	32.77	150	2016
-120.39	36.62	200	2016
-118.86	35.49	200	2016
-118.15	34.69	250	2016
-117.20	34.93	250	2016
-120.24	35.53	280	2016
-115.41	35.58	300	2016
-118.16	34.86	318	2016
-118.00	35.35	328	2016